KTH Industrial Engineering
and Management

Experimental Investigation of Refrigerant Charge Minimisation of a Small Capacity Heat Pump

Doctoral Thesis

By

W. Primal D. Fernando

Division of Applied Thermodynamics and Refrigeration
Department of Energy Technology
Royal Institute of Technology
SE-100 44 Stockholm, Sweden

Stockholm, February 2007

Trita REFR Report No. 07/58
ISSN 1102-0245
ISRN KTH/REFR/07/58-SE
ISBN 978-91-7178-569-5

Experimental Investigation of Refrigerant Charge Minimisation of a Small Capacity Heat Pump

Abstract

Enormous quantities of heat are available in air, soil, water, exhaust air from buildings, and in waste water of any kind. However these heat sources are useless for heating purposes since their temperatures are lower than the temperature required for heating. Heat pumps can be used to extract heat from these sources with a small expenditure of additional energy and up-grade and deliver the energy as useful heat for room heating. The heat pump cycle employs the well-known vapour compression cycle. The amount of heat delivered by a heat pump is equal to the amount of energy extracted from the heat source plus the heat equivalent to the compression work of the heat pump. Heat pumps, of course, are being generally accepted as outstanding energy saving units due their coefficient of performance (COP).

Heat pumps for house heating have been used extensively in many countries and are especially common in Sweden. The annual growth rate of heat pump usage in Sweden is the same as in rest of Europe. According to the Swedish heat pump association, between 1986 to August 2003, the number of installed heat pump units in Sweden was 332,309. The demand for heat pumps started to increase from the year 1995 and in the year 2002, approximately 40,000 heat pump units were installed. Among the many types available, single-family heat pumps providing heating capacity of about 5 kW are widely popular.

The main drawbacks of heat pumps are the complexity of the systems, high cost, need of technical knowledge, safety hazards and environmental effects of certain refrigerants, etc. An efficient heat pump with small refrigerant charge would have less of some of these drawbacks and could be a competitive alternative to other heating processes.

In this study, methods of refrigerant charge minimisation without reducing the performance of a small capacity (5 kW) heat pump have been investigated. Work has been focused on finding refrigerant charge distribution in different components of the heat pump, on finding out the solubility of refrigerant (propane) with different compressor lubrications oils, on testing different types of compact heat exchangers, on constructing new minichannel heat exchangers and on finding correlations for calcu-

lating the heat transfer of minichannel heat exchangers. The results included in this thesis have been presented in four conference papers and five journal papers of which two were published and three were submitted for publication.

The purpose of the work reported in *Paper I* was to find out the optimum refrigerant charge and the refrigerant charge distribution of the experimental heat pump constructed with brazed plate heat exchangers. The optimum refrigerant charge of the system was found to be 280 - 320 g for the tested conditions. The amount of refrigerant in the evaporator, condenser, liquid line and the compressor were 70 - 80 g, 100 - 130 g, 26 g, and 35 - 40 g, respectively. The amount of missing or undrained refrigerant was 35 - 40 g.

The purpose of *Paper II* was to find the optimum refrigerant charge and refrigerant charge distribution of the experimental heat pump fabricated with commercially available flat tube minichannel heat exchangers and to compare the results with those of *Paper I*. The results show a reduction of the total refrigerant charge by about 75 g and also considerable performance reduction.

The purpose of *Paper III* was to find the solubility of propane in compressor lubrication oils. The tests show that propane is more soluble in the tested POE (polyol ester) oils than PAG (polyalkylene glycol) oils.

The purpose of Paper *IV* was to compare the performances of multiport minichannel aluminium evaporator and condenser (they were constructed within the project) with the plate type heat exchangers reported in *Paper I*. The comparison shows improvements of overall heat transfer coefficients of the evaporator and condenser by 50% and 60%, respectively, reduction of refrigerant amounts in the evaporator and condenser from 69 to 28 g and 125 to 96 g, respectively, and improvements of COP1 and COP2 from 3.32 to 3.59 and 2.31 to 2.70, respectively.

In *Paper V*, the single-phase heat transfer coefficients of the multiport minichannel aluminium heat exchanger were investigated. Available correlations from the literature were compared to the experimental results and new correlations for the single-phase heat transfer of the minichannel heat exchanger were suggested.

In *Paper VI,* the evaporative heat transfer coefficients of the multiport minichannel aluminium heat exchanger were investigated. The results were compared with correlations from the literature and several compared correlations were modified in order to predict the evaporative heat transfer of the minichannel heat exchanger.

In *Paper VII,* the condensation heat transfer coefficients of the multiport minichannel aluminium heat exchanger were investigated. The results were compared with correlations from the literature and several compared correlations were modified in order to predict the condensation heat transfer of the minichannel heat exchanger.

The purpose of *Paper VIII* was to investigate the performance, optimum refrigerant charge and charge distribution of the heat pump constructed with minichannel aluminium heat exchangers, at a heat sink temperature of 40°C together with heat source temperatures of -10°C, -2°C, +6°C and +12 °C, respectively. The optimum refrigerant charge increased with increasing heat source temperature and was found to be 170, 200, 240 and 265 g, respectively. The paper also reports the variations of COP1 when the heat source temperature was varied from -12 to +12°C.

The purpose of *Paper IX* was to investigate the performance of the heat pump constructed with minichannel aluminium heat exchangers at different condensing temperatures together with varying heat sink temperatures. Minimum refrigerant charge required for stable operation at condensation temperatures of 35°C, 40°C, 50°C and 60°C was found to be 230, 224, 215, and 205 g, respectively. The paper also presents the overall performances of the scroll compressor used in the heat pump.

Key Words: heat pump, propane, low-charge, Wilson plot method, minichannels, aluminium heat exchangers, single-phase flow, single-phase heat transfer, multiport channels, shell and tube, minichannel evaporator, minichannel condenser

Acknowledgments

I am very grateful to my advisor Professor Björn Palm for his effective support, continuous encouragement and sharing his profound knowledge with me during the whole project. You always made time for people even in your vacation time, kept your doors open and it is very rare to here from you "I am busy now, come later". Without your contributions in various aspects, this thesis would not have been accomplished.

Financial support from The Swedish National Energy Administration, aluminium tube supply from Hydro Aluminium, especially Mr. Clemens Sodeik and compressor supply from Copeland is gratefully acknowledged. I would like to acknowledge Anders Hedendahl, Bo Wahlberg and Michael Lövgren from ALUMBRA for their assistance in constructing the multiport minichannel aluminium heat exchangers.

I would like to express my deep thanks and sincere appreciation to Professor Per Lundqvist for his support and valuable comments on published articles. You are a special person with many brilliant ideas. Thanks for your Skiing and Sailing lessons.

I would like to express my deep thanks and sincere appreciation to Professor emeritus Eric Granryd for his support and valuable comments on the published articles as well as the experiments. Your profound knowledge, experience and quick responses for my questions inspired my work as well as my knowledge. I am extremely proud of been able to work with a person like you and greatly appreciate your humbleness.

I would like to express my deep thanks and sincere appreciation to Klas Andersson for his help in constructing the multiport minichannel aluminium heat exchangers. Without your personal industrial contacts, these heat exchangers would not have been constructed. Then, this thesis would have been a different story.

I would like to express my deep thanks and sincere appreciation to Oxana Samoteeva for the works conducted during the project. Especially your friendly behaviour made me finding it easy to work.

The advices and support for the electrical/electronic connections and developing of the computer programmes by Dr. Joachim Claesson and Mr. Peter Hill are greatly appreciated. Also mechanical support for the construction of the test facilities by Benny Sjöberg, Benny Andersson and Bernt Wennström is greatly appreciated. Late Bo Johansson is specially remembered for his help during the test facility construction.

I would like to express my deep thanks and sincere appreciation to Martin Forssén, Jan-Erik Nowacki for information and advice given at various instances.

I would like to express my deep thanks and sincere appreciation to Professor Tim Ameel from Department of Mechanical Engineering, University of Utah, USA, for his editorial assistance, comments and advises regarding several published articles. Your help really improved my writing ability and greatly improved the quality of the publications.

Many thanks to all staff members at the Division of Applied Thermodynamics and refrigeration: Erik Björk, Raul Anton, Jaime Arias, Inga Du Rietz, Åke Melinder, Ali Rashid, Getachew Bekele, Yang Chen, Richard Furberg, Anders Johansson, Hans Jonsson, Nabil Kassem, Rahmatollah Khodabandeh, Peter Kjaerboe, Claudi Martin, Susy Mathew, Wahib Owhaib, Samer Sawalha, Marino Grozdek and also former staff members Cecilia Hägg, Wimolsiri Pridasawas, Dimitra Sakellari, Emilio Navarro, Shota Nozadze, Branko Simanic. Your smiles, talks, advices and sense of humour made it a very pleasant environment to work in.

Special thanks to Dr. Ivo Martinac and Professor Jan Blomstran for their help to continue for my studies in Sweden.

Many thanks to computer support, Tony Chapman, Birger Söderström and friends from HPT division, Jeevan Jayasuriya, Nalin Nawarathne and all others. Also, I would like to thanks friends Nameen Abeyratne and Simeon Morell who helped me at various instances of preparing this report.

I would like to express my deep thanks and sincere appreciation to our former staff member and my best friend Sanjeeva Witharana for his guidance and help to find Sweden for my education. Without your assistance this story would be very different.

Many thanks to my Father and Mother who passed away before my graduation, my brothers Percy Fernando, Laksiri Fernando and my sister Inoka Fernando for their encouragements and help.

Last but not least, I am deeply grateful to my family to whom this thesis is dedicated, my wife Dinesha for her support, sacrifices, love and understanding, my lovely daughter Stina for her love and inspiration and patience during all these years.

Preface

When I was a school kid, my main interest was playing cricket, volleyball and football. My late parents did not like that. They always asked me to study and go to additional tuition classes, after school. I liked to go to additional tuition classes since I got more freedom from my parents after the school. I left home, but hardly attended tuition classes, instead ended up playing cricket with my village team mates or playing volleyball with my school team mates. My parents got to know this when I had to go for several days away from home for inter school volleyball finals. Even though they did not feel good about it, they allowed me to go and my school team ended up becoming the national champions. Of course, my parents gave up hopes of my future education and I got exceptional freedom from my parents. After the volleyball matches, I just had only several months to study for the ordinary level examination. I worked hard a few months and passed the ordinary level exam with distinction pass for mathematics. My results astonished my parents and they promised me to give unlimited assistance, if I do my higher education or otherwise asked me to find a job without wasting their money. I decided to continue my studies in mathematics. After three years of hard work, I was selected to the faculty of engineering, at University of Moratuwa, Sri Lanka. There, I earned not only a degree, but found someone to live with for the rest of my life, of course, she is my loving wife Dinesha.

After I got my degree, I planned to work as an engineer and to stop further studies. While I was working, one day, one of my best friends, Sanjeeva, who studied in the International Master Program, in Sweden, contacted me and asked about my wiliness to join him for the following year's International Masters Program.

I arrived to Sweden with a plan to stay just for 9 months. Then it was prolonged for another 5 months. When it was three days to go back to Sri Lanka, I got this Ph.D. position, since then I am here.

During my time in Sweden, we added a lovely daughter to our family. To have all good memories, we named her with a Swedish name, Stina.

Even though, I am far-away from my beautiful warm country, I never felt loneliness in Sweden. Snow was not a big issue. I always remember our department activities that kept our colleagues more united and active. Specially, skiing, sailing, skating, boat trips, canoeing, Christmas parties and playing foot ball.

Now, I have come a long way. My thesis is submitted for a Ph.D. degree.

Publications

The present thesis is based on several previously published articles. They are:

Conference papers

These papers have been published in conference proceedings and were presented during the conference.

1. W. Primal D. Fernando, Oxana Samoteeva, Per Lundqvist, Björn Palm, Charge Distribution in a 5 kW Heat Pump Using Propane as Working Fluid - Part I: Experimental Investigation, Proc. 16. Nordiske Kølemøde og 9. Nordiske Varmepumpedage 29.-31. August 2001, København, 299 p.
2. W. Primal D. Fernando, Björn Palm, Eric Granryd, Oxana Samoteeva, Klas Anderson, The Behaviour of Small Capacity (5 kW) Heat pump With Micro-Channelled Flat Tube Heat Exchangers, Proc. Zero leakage and Minimum charge, efficient systems for refrigeration and air conditioning and heat pumps. IIR-Conf. 26-28 August, Stockholm, Sweden, 179p.
3. W. Primal D. Fernando, Houde Han, Björn Palm, Eric Granryd, Per Lundqvist, The Solubility of Propane (R290) with Commonly Used Compressor Lubrication Oils, Proc. International conference on compressors and their systems, IMechE Conference Transactions 2003-4, Professional Engineering Publishing, ISSN 1356-1448.
4. W. Primal D. Fernando, Björn Palm, Eric Granryd, Klas Andersson, Mini-channel Aluminium Heat Exchangers with Small Inside Volumes, Proc. 21st IIR International Congress of Refrigeration, Washington DC, August 17-22, 2003.

Journal papers

5. Primal Fernando, Björn Palm, Tim Ameel, Per Lundqvist, Eric Granryd, A Minichannel Aluminium Tube Heat Exchanger - Part I: Evaluation of Single-Phase Heat Transfer Coefficients by the Wilson Plot Method, Submitted to International Journal of Refrigeration, January 2007.
6. Primal Fernando, Björn Palm, Tim Ameel, Per Lundqvist, Eric Granryd, A Minichannel Aluminium Tube Heat Exchanger - Part II: Evaporator Performance with Propane, Submitted to International Journal of Refrigeration, January 2007.

7. Primal Fernando, Björn Palm, Tim Ameel, Per Lundqvist, Eric Granryd, A Minichannel Aluminium Tube Heat Exchanger - Part III: Condenser Performance with Propane, Submitted to International Journal of Refrigeration, January 2007.

8. Primal Fernando, Björn Palm, Per Lundqvist & Eric Granryd, Propane Heat Pump with Low Refrigerant Charge: Design and Laboratory Tests, International Journal of Refrigeration, Volume 27, Issue 7, November 2004, Pages 761-773.

9. Primal Fernando, Björn Palm, Per Lundqvist, Eric Granryd, Performance of a single-family heat pump at different working conditions using small quantity of propane as refrigerant, Journal of Experimental Heat Transfer, Taylor & Francis, Accepted Feb. 2006.

Internal reports

This is a literature review report and has been published under the Department Publications 2007. The access for this report is only for the people from the Department of Energy Technology, Division of Applied Thermodynamics and Refrigeration. The literature review may be requested from the Department of Energy Technology for other people.

10. Primal Fernando, Literature survey on heat pumps, refrigeration compressor lubrication oils, and for single-phase, evaporative and condensing heat transfer of minichannel heat exchangers.

Other papers

These papers have been not included in this thesis. They were published within the project from the experimental results.

Conference papers

These papers have been published in conference proceedings and were presented during the conference by the first author.

11. O. Samoteewa, **P. Fernando**, B. Palm, P. Lundquist, "Charge Distribution in a 5kW Heat Pump Using Propane as Working Fluid. Part II: Modelling of Liquid hold-up" Proceedings: 16. Nordiske Kølemøde og 9. Nordiske Varmepumpedage, Copenhagen, Denmark, August 29-31, 2001.

12. O. Samoteewa, E. Granryd, B. Palm and **P. Fernando**, "Modelling of the amount of refrigerant and pressure drop in a rectangular copper microchannel evaporator" - Proc, Zero Leakage and Minimum Charge, Efficient Systems for Refrigeration Air Conditioning and Heat pumps, IIR Conf, Stockholm, Sweden August 26-28, 2002 (page 449).

13. B. Palm, **P. Fernando**, K. Andersson, P. Lundqvist and O. Samoteeva, "Design a heat pump for minimum charge of refrigerant" , 8th International Energy Agency, Heat Pump conference 2005, Global Advances in Heat Pump Technology, Applications and Markets, Las Vegas, Nevada, USA, May 30 - June 2, 2005.

Journal papers

14. **Primal Fernando**, Per Lundqvist, Refrigeration Systems with Minimized Refrigerant Charge - System Design and Performance, Proc. IMechE Vol. 219 Part E: J. Process Mechanical Engineering, Special issue paper, pp. 127 - 137, 15 June 2004.

Industrial seminar presentations

This series of seminars are conducted in the Department of Energy Technology, Division of Applied Thermodynamics and Refrigeration, Royal Institute of Technology (KTH), SE-100 44 Stockholm, Sweden for people from the Industry.

15. Primal Fernando, O. Samoteeva, Approach to low charge refrigeration systems by heat exchanger developments, Industrial Seminar, Department of Energy Technology, Division of Applied Thermodynamics and Refrigeration, Royal Institute of Technology (KTH), SE-100 44 Stockholm, Sweden.
16. K. Andersson, P. Fernando, O. Samoteeva, Värmeväxlare med nya mikrokanaler ger liten innervolym, Industrial Seminar, Department of Energy Technology, Division of Applied Thermodynamics and Refrigeration, Royal Institute of Technology (KTH), SE-100 44 Stockholm, Sweden (2001-11-26).
17. K. Andersson, P. Fernando, O. Samoteeva, Tio tändare fyller en värmepump - Om minimering av köldmediefyllning, Industrial Seminar, Department of Energy Technology, Division of Applied Thermodynamics and Refrigeration, Royal Institute of Technology (KTH), SE-100 44 Stockholm, Sweden (2003-04-09).

Errors founds in the publications

Paper I

1. Page 92, Fig. 4, in the legend, Eva-g: refrigerant hold-up in the evaporator by grams, Liq-g: refrigerant hold-up in the liquid line by grams, Con-g: refrigerant hold-up in the condenser by grams and Gas-g: refrigerant hold-up in the condenser including discharge line, should be included in the nomenclature.

2. Page 93, line 1 "***no gas bubbles***" should be changed to "***no vapour bubbles***". Generally, in this paper, "***gas***" referred to "***refrigerant vapour***".

3. Page 94, Fig. 6, in the legend, con-tem: condensation temperature, eva-tem: evaporation temperature, Gly-in: glycol inlet (heat source) temperature of the evaporator and Con-out: cooling water outlet (heat sink) temperature of the water, should be included in the nomenclature.

Paper II

4. Page 99, title, "***micro-channelled***" should be changed to "***micro-channel***". Generally, it should be changed in all over the paper.

Paper III

5. Page 113, abstract, paragraph 2, line 2, "***in suction line***" should be changed to "***in discharge line***".

6. Page 116, Figure 1, Legend, "***Total***" is meant that the total amount of refrigerant in the suction side of the compressor.

Paper IV

7. Page 126, section 1.1, line 7, "***Length: 651 mm***" should be changed to "***Length: 661 mm (heat transfer length 651 mm)***".

8. Page 127, section 1.2 The end plates and baffle plates, line 2, "***thickness of an end plate was 5mm***" should be changed to "***thickness of an end plate of the condenser 5mm and evaporator 8 mm, respectively***".

9. Page 133, Table 2, Total heat transfer areas (m^2) 0.88 and 0.82, should be in the columns of side 2 in the respective heat exchangers.

10. Page 133, Table 3, Total heat transfer areas (m^2) 1.01 and 0.98, should be in the columns of side 2 in the respective heat exchangers.

11. Page 133, Table 2, 3, Height of the heat exchangers were given including the connection lengths.

Paper VIII

12. Page 237, section 2.2 Mini-channel aluminium heat exchangers, line 8, "***the length of each tube was 651 mm***" should be changed to "***the length each tube was 661 mm***".

13. Page 240, line 11, "***flow measurements 0.5%***" should be changed to "***flow measurements ±0.5%***".

Paper IX

14. Page 262, before last line, "***A length of a tube was 651 mm***" should be changed to "***A length of a tube was 661 mm***".

15. Page 264, line 9, "***flow meters were given as 0.5%***" should be changed to "***flow meters were given as ±0.5%***".

Nomenclature

A	area (m^2)
AWG	American wire gage
ANSI	American national standard institute
AAD	absolute average deviation
CH	channel
COP	coefficient of performance
Con	condenser
c/c	centre-to-centre
D, d	diameter (m)
DP1, DP2	differential pressure gauges
DPT	differential pressure transducer
Eva	evaporator
Exp	experimental
f	friction factor
GWP	global warming potential
$G\tilde{z}$	Gratz number
G	mass flux (kg m^{-2} s^{-1})
H.T.C	heat transfer coefficient ($Wm^{-2}.K^{-1}$)
H	high
HFC	hydrofluorocarbon
ISO	International Standard Organization
k	thermal conductivity ($Wm^{-1}K^{-1}$)
L, X	channel length (m)
L	low
l	sectional length (m)
Liq	liquid
LMTD	log mean temperature difference (K)
MCFT	mini channel flat tube heat exchanger
M	Mach number of fluid
$M(x)$	Mach number at a distance x from inlet
MAE	mean absolute error
N	number of measured values
Nu	Nusselt number
$\overline{Nu}$	average Nusselt number
Nu_∞	Nusselt number at fully develop flow
ODP	ozone depletion potential
p	pressure (Pa), wetted perimeter (m)
P	pressure meter
P1, P2	pressure gauges
Pr	Prandtl number
PAG	polyalkylene glycol
POE	polyol ester

Pre	predicted
PT	pressure transducer
q	local heat flux (Wm^{-2})
q_w	wall heat flux (Wm^{-2})
$\dot{Q}$	heat rate (W)
Re	Reynolds number
R	radius (m)
r	uncertainty due to random errors
SL	Select Lubricants
T1, T2,….T10	Thermocouples
t	temperature (°C)
t	factor depending on confidence level (Student t-factor)
T	thermocouple
u	local velocity of the fluid (ms^{-1})
U	overall heat transfer coefficient ($Wm^{-2}K^{-1}$)
U	overall uncertainty
V1, V2,…V4	pneumatically operated ball valves (stop-valves)
w	systematic error (type B)
x	quality
$\bar{x}$	mean value
x_i	measured values (variables)

Greek symbols

α	convective heat transfer coefficient ($Wm^{-2}K^{-1}$)
$\overline{\alpha}$	average heat transfer coefficient ($W\ m^{-2}\ K^{-1}$)
β	confidence level (%)
δ	thickness (m)
η	efficiency
μ	dynamic viscosity ($kgm^{-1}s^{-1}$)
ξ	fin efficiency
ρ	local density of the fluid along the channel (kgm^{-3})
ρ_0	density of the fluid at channel inlet (kgm^{-3})
σ	standard deviation of the population
σ_x	standard deviation of the sample
$\sigma_{\bar{x}}$	standard deviation of the mean value (standard error)

Subscripts

b	base
f	fin
fd,h	hydrodynamically fully developed
fd,t	thermally fully developed
h	hydraulic
H	hermetic

m	mean
r	refrigerant
s	surface
t	tube
0	initial
1	condenser, refrigerant side
2	evaporator, water side

Experimental Investigation of Refrigerant Charge Minimisation of a Small Capacity Heat Pump

1 Introduction

1.1 Motivation and objectives

Demand for refrigeration, air-conditioning and heat pump equipment has been increasing dramatically in the past few decades. Simultaneously, the environmental impacts associated with the release to the open environment of the synthetic refrigerants used in the majority of these plants have come into focus. The ozone depletion potential (ODP) and global warming potential (GWP) of many of these refrigerants are the major environmental concerns. Different fluids naturally occurring in the environment have been suggested and tested as refrigerants, due to their much lower environmental impact. One group of such natural fluids are the hydrocarbons. The thermodynamic and transport properties of these fluids are favourable, but the flammability is a major concern. However, the risks are dependent on the concentration of refrigerant in a particular space. Therefore, it is important to maintain the refrigerant quantity in a system as small as possible.

Natural refrigerants are by many considered as the best candidates for the future due to their low environmental impact compared to synthetic refrigerants. Particularly, the environmental effects of synthetic substances are still not completely known as the possible interactions with the environment are almost infinite. Therefore, research interest during the last decades has been focused on applications of well characterized natural refrigerants. Propane is one of the substances being considered. It is a natural refrigerant that does not have any ozone depletion potential and has a very low global warming effect compared to most commercially available synthetic refrigerants. It is non-toxic, chemically stable while inside the refrigeration system, compatible with most materials used in Hydro-Fluoro-Carbon (HFC) equipments and miscible with commonly used compressor lubricants. Propane has very good thermodynamic and transport properties and also properties that closely resemble HFC refrigerants, allowing it to be used without re-design of existing systems. However, the main concern with the use of propane as refrigerant is its high flammability. To reduce the risks using propane or other flammable refrigerants, it is important to reduce the charge of refrigerant necessary to operate a system. A low charge is also beneficial from an environmental point of view when using HFC refrigerants as it will reduce the leakages to the atmosphere.

Refrigeration and air-conditioning systems that are designed to operate with small refrigerant charges and zero refrigerant leaks may avoid the risk of the flammability. The specific volume of propane is higher than that of the HFC refrigerants. Therefore, a refrigeration system that operates with propane contains less refrigerant mass than the same system operated with HFCs.

The refrigerant charge of a heat pump or refrigeration system is strongly connected to the total internal volume of the system, including the volumes of tubes, compressor and heat exchangers. Refrigeration systems designed with short tubing, small volume receivers and compact heat exchangers will have a dramatically reduced internal volume as well as mass of refrigerant compared to a typical standard system.

Several types of compact heat exchangers are widely employed in small refrigeration, air-conditioning and heat pump systems. Among them, plate-type heat exchangers are one of the most popular due to their high heat transfer area to internal volume ratio and their good performance.

Recent advances in manufacturing technologies for small channel diameter aluminium tubes allow the construction of even more compact heat exchangers than plate-type. It is well known that the reduction of the channel diameter increases the heat transfer coefficient for a given mass flux. Various types of aluminium tubes are available in the market: Multiport tubes, tubes with inside fins, different geometries, etc. These types of new tubes provide opportunities to design new extremely compact heat exchangers.

The objective of the present thesis is to experimentally investigate, how to minimise the refrigerant charge of a small capacity liquid-to-liquid heat pump with the goal of reaching a charge of less than 150 g. The minimum heating capacity of the heat pump (condenser capacity) should be 5kW at typical running conditions.

1.2 Method

The method used in the present study is primarily experimental. The reason for this choice is that available correlations and calculation methods for determining heat transfer, pressure drop and, most important for this study, void fractions in two-phase flow are not accurate enough to be used as a basis for determining the performance and the refrigerant charge of a refrigeration or heat pump system. This is particularly true for the performance and refrigerant inventory of minichannel heat exchangers, which were of central importance in the present study.

For the experimental investigation a test-rig was built, designed to simulate a heating-only, liquid-to-liquid heat pump, the type most frequently used in Sweden. A glycol solution was used for the secondary refrigerant loop of the evaporator and water was used as secondary refrigerant of the condenser loop. The thermo-physical properties of water and glycol were evaluated by using MS Excel subroutines developed by Melinder (1997).

The working fluid (refrigerant) in all tests was propane. Thermo-physical and transport properties of propane were evaluated in MS Excel with Refprop 6.01 code (NIST 1998) and with Refprop 7.0 code (NIST 2002).

A Copeland scroll-compressor was used throughout the investigation. The compressor contained about 1.2 l of ester-type lubrication oil. Information about oil circulation in the system was not available.

Initially, the test-rig was constructed using a thermostatic expansion valve. Due to adjustment difficulties of the valve for various test conditions, it was later replaced by an electronic expansion valve.

Commercial brazed-plate-type heat exchangers were used as evaporator and condenser of the initial tests. Later, the plate-type heat exchangers were replaced by commercial heat exchangers with rectangular shaped minichannel copper tubes. Finally, the copper-tube heat exchangers were replaced by prototype heat exchangers designed within the project. These heat exchangers were made from commercially available multiport minichannel aluminium tubes.

The performances of the brazed plate and copper-tube heat exchangers were evaluated only in terms of the overall heat transfer coefficients. A separate test-rig was built in order to investigate the shell-side (secondary side) single-phase heat transfer coefficients of the mini-channel aluminium heat exchanger. This allowed detailed investigations of the evaporative and condensation heat transfer coefficients of the multiport minichannel heat exchangers.

Tests with plate-type heat exchangers were made under the following test conditions: Glycol inlet temperatures of the evaporator approximately from -1 to -3°C (evaporation temperature around -8 to -9°C) and water outlet temperatures of the condenser approximately from 39 to 40°C (condensing temperature around 40 to 41°C).

Tests with rectangular copper-tube heat exchangers were made under the following test conditions: Evaporation temperatures of -16, -8, 0 and

+5°C and water outlet temperatures of the condenser approximately from 39 to 40°C (condensing temperature around 40 to 41°C).

Tests with multiport minichannel aluminium heat exchangers were made under the following test conditions: Evaporation temperatures from -16 to +15°C and condensing temperatures from 30 to 60°C.

The first sets of tests were focused on experimentally investigating the refrigerant charge distribution in various parts of the refrigerant loop of the heat pump. For this purpose, four ball valves, which could be operated either manually or pneumatically, were placed in the connecting tubes between each of the main components. The tube lengths of the refrigerant circuit were kept as short as practically possible. An electrically heated glycol solution circulated in a closed loop through the secondary side of the evaporator in opposite direction to the refrigerant flow and supplied the heat load for the evaporator. The cooling water that circulated on the secondary side of the condenser in opposite direction to the refrigerant flow was cooled by a cold water tank.

To determine the influence of the refrigerant charge on the performance, and to find the charge giving the highest coefficient of performance (COP), the following procedure was used: A certain amount of propane (amount just needed for operation) was charged into the heat pump and set in operation. The condensation or heat sink temperature was maintained at a given constant level and at the same time, either the evaporation temperature or heat source temperature was maintained at a desired value. The refrigerant charge in the system was then increased in steps while maintaining the above conditions at the given values. The total refrigerant charge in the system was noted down and performance measurements were done at stable conditions. The coefficient of performance (COP) of the heat pump was calculated for each change in refrigerant charge. The refrigerant charge of the system at maximum COP was considered as the optimum refrigerant charge of the system for the tested conditions. The heat pump was then filled with this optimum refrigerant charge for the tested conditions and set in operation. At stable running conditions, the pneumatically operated ball valves were closed all at once so that the refrigerant was locked into the condenser, evaporator, compressor or liquid line (expansion valve included in the liquid line). Then, the refrigerant in the different parts was separately drained into an externally connected cylinder. The cylinder was vacuumed before use and connected to the system via a flexible tube and the cylinder was immersed in a liquid-air-bath. By doing this, all refrigerant in the different sections was drained into the cylinder separately and weighed.

The various types of heat exchangers noted above were connected to the heat pump and refrigerant charge distributions in different parts with those heat exchangers were investigated. From the experience gained from above experiments, three multiport minichannel heat exchangers (shell-and-tube-type) were designed. Single-phase heat transfer coefficients of the shell and tube-side, evaporation heat transfer coefficients of the tube-side and condensation heat transfer coefficients of the tube-side of the designed heat exchangers were investigated and compared with correlations from the literature. In this way, suitable correlations for determining the heat transfer coefficients of the minichannel aluminium heat exchangers were identified.

Experiments were also conducted in order to investigate the solubility of propane with various types of commercially used compressor lubrication oils. Suitable compressor lubrication oil types for use with propane were proposed.

An extensive literature survey has also been conducted. This survey includes heat pumps, lubrication oils, and single-phase, evaporation and condensation heat transfer in minichannel heat exchangers.

2 Summaries of the Publications

2.1 Introduction

The present thesis is based on nine articles which have been written during the course of the project. Of these, six have been published in scientific journals or presented at international conferences. The remaining three have recently been submitted to scientific journals for publication. Beside these articles, a comprehensive literature survey has been conducted and presented in an internal report at the Department of Energy Technology, Royal Institute of Technology (KTH). The nine articles are attached as appendices to the thesis. The literature review may be requested from the Department of Energy Technology.

List of publications included in this thesis,

Conference papers

1. W. Primal D. Fernando, Oxana Samoteeva, Per Lundqvist, Björn Palm, Charge Distribution in a 5 kW Heat Pump Using Propane as Working Fluid - Part I: Experimental Investigation, Proc. 16. Nordiske Kølemøde og 9. Nordiske Varmepumpedage 29.-31. August 2001, København, 299 p.
2. W. Primal D. Fernando, Björn Palm, Eric Granryd, Oxana Samoteeva, Klas Anderson, The Behaviour of Small Capacity (5 kW) Heat pump With Micro-Channelled Flat Tube Heat Exchangers, Proc. Zero leakage and Minimum charge, efficient systems for refrigeration and air conditioning and heat pumps. IIR-Conf. 26-28 August, Stockholm, Sweden, 179p.
3. W. Primal D. Fernando, Houde Han, Björn Palm, Eric Granryd, Per Lundqvist, The Solubility of Propane (R290) with Commonly Used Compressor Lubrication Oils, Proc. International conference on compressors and their systems, IMechE Conference Transactions 2003-4, Professional Engineering Publishing, ISSN 1356-1448.

4. W. Primal D. Fernando, Björn Palm, Eric Granryd, Klas Andersson, Mini-channel Aluminium Heat Exchangers with Small Inside Volumes, Proc. 21st IIR International Congress of Refrigeration, Washington DC, August 17-22, 2003.

Journal papers

5. Primal Fernando, Björn Palm, Tim Ameel, Per Lundqvist, Eric Granryd, A Minichannel Aluminium Tube Heat Exchanger - Part I: Evaluation of Single-Phase Heat Transfer Coefficients by the Wilson Plot Method, Submitted to International Journal of Refrigeration, January 2007.
6. Primal Fernando, Björn Palm, Tim Ameel, Per Lundqvist, Eric Granryd, A Minichannel Aluminium Tube Heat Exchanger - Part II: Evaporator Performance with Propane, Submitted to International Journal of Refrigeration, January 2007.
7. Primal Fernando, Björn Palm, Tim Ameel, Per Lundqvist, Eric Granryd, A Minichannel Aluminium Tube Heat Exchanger - Part III: Condenser Performance with Propane, Submitted to International Journal of Refrigeration, January 2007.
8. Primal Fernando, Björn Palm, Per Lundqvist & Eric Granryd, Propane Heat Pump with Low Refrigerant Charge: Design and Laboratory Tests, International Journal of Refrigeration, Volume 27, Issue 7, November 2004, Pages 761-773.
9. Primal Fernando, Björn Palm, Per Lundqvist, Eric Granryd, Performance of a single-family heat pump at different working conditions using small quantity of propane as refrigerant, Journal of Experimental Heat Transfer, Taylor & Francis, Accepted Feb. 2006.

The nine articles included in the thesis were prepared in order to answer the following questions raised on the title of the thesis, "Experimental Investigation of Refrigerant Charge Minimisation of a Small Capacity Heat Pump".

1. How is the refrigerant distributed within the refrigerant circuit of the heat pump?
2. Can the refrigerant charge be reduced by introducing minichannel heat exchangers?
3. Is it possible to decrease the refrigerant charge by changing the compressor lubrication oil?
4. Is it possible to design more compact heat exchangers than those available in the market and how the performance of the newly designed heat exchangers compared to those is available on the market?

5. Are the available correlations for single-phase heat transfer from the literature valid for the newly designed heat exchanger?
6. Are the available correlations for evaporative heat transfer from the literature valid for the newly designed heat exchanger?
7. Are the available correlations for condensation heat transfer from the literature valid for the newly designed heat exchanger?
8. What is the optimum refrigerant charge of the heat pump with the newly designed heat exchangers? How is the performance of the heat pump at the optimum charge with the newly designed heat exchangers?
9. How does the performance of the heat pump vary with the refrigerant charge for given heat source and heat sink temperatures?

The remainder of this chapter contains a short summary of the literature survey and summaries of the attached articles in this thesis.

2.2 Summary of the literature survey

An extensive literature survey was conducted for finding information on heat pumps, refrigeration compressor lubrication oils, and for single-phase, evaporative and condensation heat transfer of minichannel heat exchangers. This survey has been reported in an over 100-page report, primarily intended for internal use at the department. The main findings of the survey are presented below.

2.2.1 Heat pumps

The heating demand of a house is dependent on many factors, such as size of the house, number of occupants, location of the house, insulation level of the house, climate conditions, etc. For the good performance of the heat pump, the heat source temperature, heat extraction method from that heat source as well as the temperature and heat delivery method to the house are of prime importance. Various types of heat sources, their applicability, advantages and disadvantages are presented in the literature survey. A conclusion of the literature survey is that the ground is a preferable heat source compared to other types of heat sources. The reason for this is the stable and relatively high temperature of the ground, as well as the infinite supply and general availability.

Concerning the various types of heating systems, floor heating provide the highest COP in heat pump applications compared to other heating systems. The main reason for that is the low distribution temperatures needed for heating with this type of system.

Table 2.1. Summary of primary and heating energy demands of a house reported in the literature survey section.

Reference	Description: Location	Energy Demand kWh/(m²yr)	
		Primary	Heating
Matrosv [1]	Russia – Wooden panel house	600 - 800	
Matrosv [1]	Germany	250	
Matrosv [1]	Germany – efficient house	90 - 120	
Matrosv [1]	Germany – experimental house	50 - 70	
Matrosv [1]	Sweden	135	
Chwieduk [2]	Poland		90 - 120
Balaras [3]	Denmark – energy audit (mean)		144.1
Balaras [3]	France – energy audit (mean)		110
Balaras [3]	Hellas – energy audit (mean)		108.1
Balaras [3]	Poland – energy audit (mean)		261
Balaras [3]	Switzerland – energy audit (mean)		172
Simonson [4]	Finland – ecological house	162	76
Simonson [4]	Finland – typical house	233	120
Olofsson [5]	Sweden – 700 km north Stockholm	120 - 270	70 -160
Forsén [6]	Sweden-170 km south-west Stockholm		179
Svensson [7]	Sweden-170 km south Stockholm		163
Balaras [8]	Eastern and Central Europe	250 - 400	
Balaras [8]	OECD counties	150 - 230	
Balaras [8]	Scandinavian countries	120 - 150	
Balaras [3] Herant [9]	France - 1973 France - 1998 (regulations 1975)	325 180.6	
Balaras [3] Doc.[10]	Germany – medium size (a regulation)		70
Balaras [3] Lalas [11]	Hellas- houses before 1980 Hellas-apartment before 1980 Hellas - houses (currently estimated) Hellas - apartment (currently estimated)		140 96 92 - 123 75 - 94
Balaras [3] Roulet [12]	Switzerland - before the energy norm Switzerland - after the energy norm	220 120	
Balaras [3] Chwieduk [13]	Poland - old buildings Poland - new standards		240 - 300 90 - 120
Balaras [3] Schnieders [14]	High performance (passive) housing - heating loads does not exceed 10 W/m² by means of a compact form, 221 dwellings in Germany, Sweden, Austria, Switzerland and France		15 - 20
Hastings [15]	Swiss "Minergie" and German "Niedri-genergie" standards		30
Bøhm [16]	Denmark- Copenhagen-1941		78.5

Summary of the primary and heating energy demands of single-family houses in various countries from the literature survey is shown in Table 2.1. The heating energy demand of a house is greatly dependent on climate conditions and housing standard of a country. Newly implemented energy regulations have dramatically brought down the heating demands in many countries. It has been reported that the heating demands of

some well insulated and tight houses located in Germany, Sweden, Austria, Switzerland and France are as low as 15 to 30 kWh/(m^2 yr) and that the peak power demand does not exceed 10 W/m^2. [3, 14, 15]

In general, the heating demands of many newer single-family houses in Sweden is approximately from 100 to 150 kWh/(m^2 yr). That heating energy demand can be easily fulfilled by a small capacity heat pump (5 to 7 kW). The annual average COPs of reported heat pumps are generally close to a value of 3 and further improvement of the COPs of many of those heat pumps are possible by proper installation and selection of components (especially secondary refrigerant flow pumps).

2.2.2 Refrigeration compressor lubrication oils

The literature survey contains a chapter discussing lubricants in general and specifically the lubricants used with propane. Various types of compressors and refrigerants are used in refrigeration and air-conditioning applications. Proper compressor lubrication plays an important role for performance and lifetime of a refrigeration system. The lubrication oil type used is very important, regarding the efficiency and life of the system. The type of the lubrication oil used in a compressor is mainly dependent on compressor type and refrigerant.

Viscosity or oils resistance to the flow is the most important property of lubricating oil. Thinner oils have low viscosities and thicker oils have higher viscosities. The ISO (International Standard Organization) viscosity grade is the most accepted standard today. It is very important to maintain the specified viscosity grade for a compressor for proper lubrication. The viscosities of lubricants usually vary with temperature. The refrigeration compressors are normally operated in different temperatures. Therefore, it is very important to consider the operating temperature and pressure range of the compressor oil, when determining the proper viscosity grade. The lowest viscosity of the selected compressor oil in the operating temperature and pressure range should give the necessary lubrication requirements [17].

It is well known that the refrigerant gas leaving from a compressor takes away some lubricant which will circulate through the system. The solubility of refrigerant in the lubricant is positive to some extend as it helps carrying back this oil to the compressor. However, higher solubility will cause the reduction of the viscosity of the lubricant, resulting poor compressor lubrication. Propane has a high solubility with commonly used compressor lubrication oils. Usually lubrication oil with higher viscosity grade has lower solubility with refrigerants. Variation of solubility of propane gas in two different naphthene oils (viscosities 32 and 108 mm^{2}s^{-1}) with temperature is shown in Fig. 2.1. Dotted lines represent the solubil-

ity of higher (108 mm^2s^{-1}) viscosity naphthene oil and the others represent the solubility of lower (32 mm^2s^{-1}) viscosity naphthene oil.

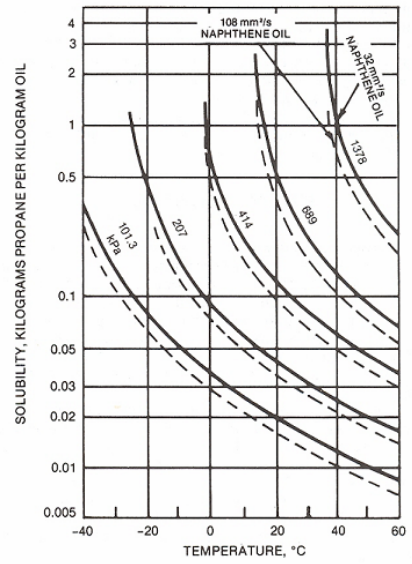

Fig. 2.1. Solubility of propane in naphthene oil [17].

The vapour pressure curve of propane is very similar to that of R22. For that reason, propane has been proposed to replace R22 in existing refrigeration systems. Furthermore, the lubrication oils that are compatible with R22 are generally compatible with propane as well. However, in case of replacement of R22 by propane in an existing refrigeration system, it is also recommended to replace the existing compressor lubrication oil by that has a higher viscosity, in order to compensate for the decrease of the viscosity by dissolving propane in the lubrication oil [18].

Some commercial lubricant manufactures have proposed several lubrication oil types for propane compressors. *Select lubricants* (SL) has recommended lubrication oils with the trade names of SL18-Series (Synthetic hydrocarbon base) and SL34-Series (Polyoxyalkylene Glycol) for natural gas and propane compressors [19]. *CPI Engineering Services* has recommended lubrication oil with the trade name of CPI-1518-Series (polyglycols based) for propane compressors [20].

2.2.3 Single-phase heat transfer and pressure drop in microchannel heat exchangers

The literature survey contains a chapter on single-phase (gas and liquid) heat transfer and pressure drop in microchannel heat exchangers. Here, channel diameters below 200 μm have been considered as microchan-

nels. For the literature survey, most recent experimental, theoretical and survey papers were considered. Not all, but a considerable number of reports state that the heat transfer and pressure drop of microchannels deviate from classical theories. However, the literature is still not conclusive, and in more recent reports, the deviations in some of the older reports are often explained by the experimental difficulties on working with small diameter channels.

Several reasons for the reported deviations from classical behaviour have been discussed in the open literature. The most important of these are gas rarefaction, surface roughness effects, effect of the entrance length, axial conduction, etc. In some of the more recent reports the fact that these effects are not taken into account in some of the previous works are suggested as the cause of deviations of the heat transfer and pressure drop of microchannels from the classical theory.

The density of gas along the flow path in normal-size tubes is usually assumed as constant when the Mach number is much less than unity. The flow becomes fully developed if the length/diameter ratio of the tube is large enough and the product of the friction factor to Reynolds number becomes constant in the laminar flow regime. Guo and Wu [21, 22] reported that the density variation along the flow direction of a microchannel might become very large if the surface friction induced pressure drop per tube length is much larger than that for conventional tubes. By numerically solving the governing equation for compressible flow in a circular tube, Guo *et al.* [23] presented the pressure and density variations along a microtube for isothermal air flow at different inlet Mach numbers. Pressure and density (relative to their inlet values) variations along the flow direction in a microtube for different channel inlet Mach numbers are shown in Fig. 2.2 [23].

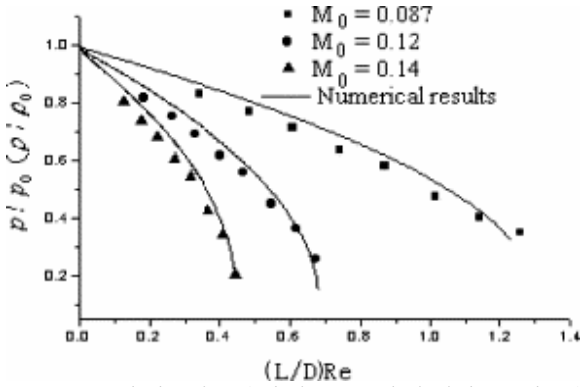

Fig. 2.2. Pressure and density (relative to their inlet values) variations along the flow direction of a microchannel [23].

Assuming a constant flow rate along a channel,

$$\rho_0 u_0 A_{cross} = \rho u A_{cross} \Rightarrow u = \left(\frac{\rho_0}{\rho}\right) u_0 \tag{2.1}$$

Since the $\left(\frac{\rho_0}{\rho}\right)$ term increases along the channel length (Fig. 2.2), the Mach number should be increased along the channel and may become very large at the channel outlet. Since the velocity is changing along the channel, no fully developed velocity or temperature profile will occur. Guo *et al.* [23] further claimed that the work due to expansion of gas leads to decrease the temperature in the channel interior, while viscous dissipation results in gas temperature rise in the near wall region leading to high heat transfer. The conventionally defined heat transfer coefficient may even be negative at the end of the channel as shown in Fig. 2.3, if the Mach number increase and the resulting temperature decrease in the channel interior are large enough.

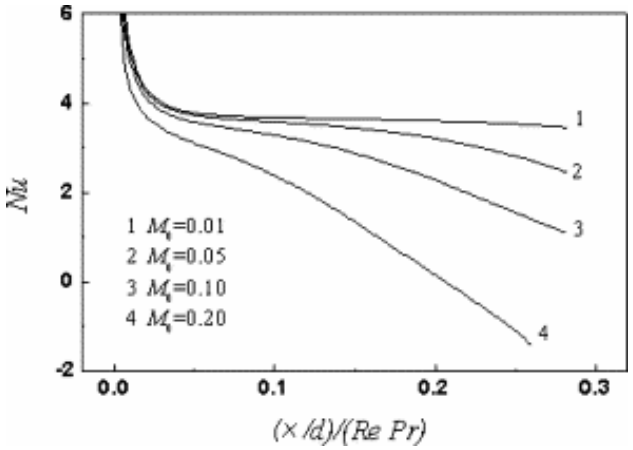

Fig. 2.3. Variation of Nusselt number along a microchannel [23].

Kohl *et al.* [24] claimed that the early transition to turbulence observed by previous reporters might have been caused by improper accounting of the effects of developing flow in the entrance region. Furthermore, they [24] proposed to include the developing flow effect when calculating the pressure drop across the channel. Friction factor data for water flow in a channel with the diameter 99.8 μm incorporating the effects of developing flow is shown in Fig. 2.4.

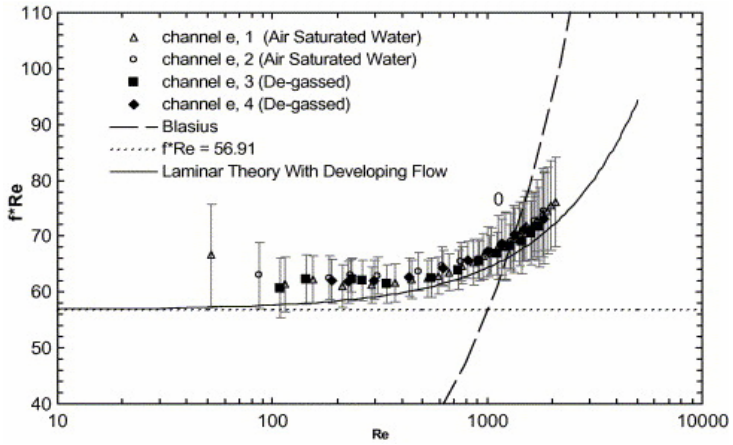

Fig. 2.4. Friction factor data for water flow in a channel with diameter 99.8 μm (the analytical prediction of *fRe* based on Shah and London [25] is 56.91; the solid line is the analytical prediction which incorporates the effects of developing flow) [24].

The generalised mean Nusselt number including the effect of thermal entry length can be written as follows [24],

$$\overline{Nu} = Nu_{\infty} + K_1 \frac{Gz}{(1 + K_2 Gz^b)} \tag{2.2}$$

where, K_1, K_2 and b are constant values. $Gz = Re\,Pr\,\frac{D}{x}$

Thermally fully developed flow is achieved when, $Gz < 10$.

For low Reynolds numbers the mean value of the Nusselt number coincide with the fully develop value, as the entrance region is very short and the effect of the viscous dissipation is not important in this flow. On the contrary, at low Reynolds numbers the effect of conjugate heat transfer on the mean value of on the Nusselt number may become very important because conduction along the channel wall becomes a competitive mechanism of heat transfer with respect to internal convection [26].

In conclusion, for laminar flow, the results of the literature survey are less conclusive. Deviations in heat transfer in the laminar flow range could be expected due to various reasons. However, no deviations are expected as long as the flow is turbulent.

2.2.4 Evaporative heat transfer in micro or minichannel heat exchangers

The review contains several papers from the literature on evaporation heat transfer inside micro and minichannels. This includes some important review-papers with summaries and author's conclusions regarding the applicability of general correlations published in the literature. It is also presented some widely used correlations for heat transfer from the literature, their validity ranges, test conditions, their accuracy limits, etc.

Many authors have reported that the heat transfer coefficient in flow boiling in micro or minichannels is dependent on the heat flux and the pressure level, but less dependent on the mass flux. This behaviour is typical for nucleate boiling and some authors therefore suggest that nucleate boiling as the dominant heat transfer mechanism in micro and minichannels. At lower flow rates, pressure fluctuations and instability of the systems have been observed.

Table 2.2. Summary of comparisons with correlations from the literature.

Test conditions	Reference & Compared Correlations	Deviations %
d_h : 0. 78 to 6 mm q : 2.95 - 2511 kWm^{-2} G : 23.4 - 2939 kgm^{-2}s^{-1} {water, R11, R12, R113}	Zhang *et al.* [27] Chen [28] Gungor - Winterton [29] Kandlikar [30] Steiner - Taborek [31] Liu - Winterton [32] Shah [33]	 9.6 - 42 *(mean 20.1)* 15.1 - 118.7 *(mean 37.3)* 11.4 - 59.7 *(mean 23.2)* 25.4 -152.4 *(mean 66.0)* 8.6 - 35.9 *(mean 21.8)* 7.7 - 77.1 *(mean 26.6)*
d : 9.52 mm q : 27 - 52 kW m^{-2} G : 170 - 460 kgm^{-2} s^{-1} {Isceon59, R407C, 404A}	Boissieux [34] Gungor - Winterton [29] Shah [33]	 Under predict Max. 80% over predict (ave. 50%)
d : 0.227 mm q : 28 - 445 kW m^{-2} G : 41 - 302 kgm^{-2} s^{-1} {water}	Koşar *et al.* [35] Kandlikar [30]	 -25.2% at lower (41 kgm^{-2} s^{-1}) mass fluxes + 35 % at higher mass fluxes (166 kgm^{-2} s^{-1})
d : 1.33 mm q : 27 - 160 kW m^{-2} G : 57 - 211 kgm^{-2} s^{-1} x : 0 – 0.3 inlet subcooling: 1 - 12K {water}	Wen *et al.* [36] Liu - Winterton [32] Chen [28] Cooper [37] Lazarek - Black [38] Tran *et al.* [39] Warrier *et al.* [40] Kenning - Cooper [41]	 MAE 28% (under) MAE 46% (under) MAE 70% (under) MAE 58% (under) MAE 245% (over) MAE 54% (under) MAE 45% (under)

d :7.75 mm q : 4.1 - 28.6 kW m^{-2} G : 240 - 1060 kgm^{-2} s^{-1} { R32, R134a, R32/134a, R-407C}	Choi *et al* [42] Gungor and Winterton [43] Gungor and Winterton [29] Kandlikar [30]	 AAD 26.4% AAD 37.6% AAD 17.6%

A summary of comparisons with correlations from the literature reported in the literature survey are shown in Table 2.2. None of the correlations in the literature for flow boiling in larger diameter channels satisfactorily predicts the heat transfer coefficients in microchannels in general and also their applicability is limited. It is therefore not possible at present to suggest a particular correlation for this application. The available correlations should be tested against more experimental data.

2.2.5 Condensation heat transfer in micro or minichannel heat exchangers

The process by which a vapour is converted to a liquid is called condensation. In general, vapour will condensate to liquid when it is cooled sufficiently by contact with a solid or another fluid that is below the saturation temperature of the condensing vapour. A significant amount of energy can be released during the condensation process due to large internal energy difference between the liquid and gas states and it is one of the most important heat transfer mechanisms. In the literature of two-phase flows, there is a large difference between the reported research woks on condensation and evaporation. In other words, research into condensation is under-represented compared to evaporation. It is only in recent years, that research on force convection condensation has been increased.

Four basic condensation mechanisms are generally recognised: Filmwise, homogeneous, dropwise and immiscible-liquid (direct contact) condensation. However, filmwise condensation is the main mode of condensation in the refrigeration industry. In filmwise condensation, the heat transfer is governed by the thickness of the liquid film at the cooled surface. Fundamentally, there are two mechanisms that are controlling the flow of condensing fluid flowing inside a tube, and thereby the film thickness. They are gravity-control conditions in which the film thickness is determined by a balance between gravity forces acting on the liquid and the shear forces at the channel wall, and vapour shear-control conditions, in which the shear forces at the liquid-vapour interface determine the film thickness. In the gravity dominated flow regime, the dominant heat transfer mode is laminar flow condensation. The heat transfer coefficient of this regime is characterized by wall-to-refrigerant temperature difference and is nearly independent of mass flux. In the shear-dominated

flow regime, turbulent condensation is the dominant heat transfer mechanism. The heat transfer coefficient of this regime is characterised by mass flux and quality.

Several well-known empirical, semi-empirical and analytical correlations from the literature are tabulated and discussed in the literature survey. Some recent research works reported in the literature are also presented. A summary of comparisons with correlations from the literature reported in the literature survey are shown in Table 2.3.

Table 2.3. Summary of comparisons with correlations from the literature.

Test conditions	Reference & Compared Correlations	Deviations %
d_h : 8 mm, G : 125 - 400 kgm^{-2}s^{-1} L : 3.67m, horizontal *inlet x* :0.9, *exit x* :0.1 Con. Tem. 30 – 50°C { HFC-134a and CFC-12}	Eckels *et al.* [44] Shah [45] Traviss *et al.* [46] Cavallini -Zecchin [47]	Correlated well within the error band of $\pm 25\%$
d_h : 2 mm q : 10 - 20 kWm^{-2} G : 100 - 200 kgm^{-2}s^{-1} L : 0.2 m, horizontal Con. Tem. 25 - 50°C, { R134a }	Yan and Lin [48] Eckels *et al.* [44]	10% higher than that of large diameter tubes (inner diameter greater than 8mm)
d_h : 8 mm, Q : 1 - 3 kW G : 50 - 350 kgm^{-2}s^{-1} L : 9.6 m, horizontal {propane, isobutane, butane and propylene binary mixtures}	Chang *et al.* [49] They modified Shah [45]	Correlated well within the error band of $\pm 20\%$
d_h : 3/8" L : 4 m { Isceon 59, R407C, R404A }	Boissieux *et al.* [50] Dobson - Chato [51] Shah [45]	Average standard deviation of 7.6%. overall standard deviation of 9.1%
d_h : 1.46 mm G : 75 - 750 kgm^{-2}s^{-1} L : 61 mm, horizontal *inlet* x : 0.03 - 0.94 Inlet. Tem. 61.5 - 66°C { HFC-134a }	Wang *et al.* [52] Akers - Rosson [53]	Mean deviation of 15.2% 83.7% of data were predicted within ±25%
d_h : 1.564 and 2.637 mm q : 4 - 12 kWm^{-2} G : 400 - 1400 kgm^{-2}s^{-1} x :0.12 -0.97, { R12}	Yang - Webb [54] Akers *et al.* [55]	Agreed well at low G At high G over predicted the data by 10 - 20%

d_h : 1.41, 1.56 mm q : 5 - 15 kWm^{-2} G : 200 - 600 kgm^{-2}s^{-1} { R410A }	Kim *et al.* [56] Web [57] Koyama *et al.* [58] Akers *et al.* [55] Shah [45]	 Within ±30% Within ±30% Within ±30% Over predicted
d_h :0.807, 1.114 mm p : 1.7 MPa G : 100 - 700 kgm^{-2}s^{-1} L : 600 mm, horizontal x :0 – 1, { R134a }	Koyama *et al.* [59] Moser *et al.* [60] Haraguchi *et al.* [61]	 Agreed well at high G Similar trend
d_h : 2.46 mm q : 5.2 kWm^{-2} G : 205 - 510 kgm^{-2}s^{-1} x : 0.15 - 0.84 {R600, R600/R290 (50 wt. %/50 wt. %), R290}	Wen *et all.* [62] Shah [45] Cavallini - Zecchin [47] Cavallini *et al.* [63] Dobson and Chato [51]	 Mean deviation 21.35 Mean deviation 25.4 Mean deviation 15.6 Mean deviation 12.8
d_h : 8 , 10.92mm G : 62 - 150 kgm^{-2}s^{-1} G : 150 - 300 kgm^{-2}s^{-1} L : horizontal, x : 0 - 1 Con. Tem. 35 - 45°C {R1270, R290, 600a, R22}	Lee *et al.* [64] Shah [45] Traviss [46] Cavallini - Zecchin [47]	 Well within ±20% Well within ±20% Well within ±20%
d_h :0.691mm q : 5 - 20 kWm^{-2} G : 100 - 600 kgm^{-2}s^{-1} L : 171 mm, horizontal x : 0.15 - 0.85 Con. Tem. 40°C, {R134a}	Shin *et al.* [65] Shah [45] Akers *et al.* [55]	 Good agreement in mass flux 200 - 600 kg/m^2 Under predicts

In the literature, the condensation heat transfer inside horizontal circular tubes with diameters greater than 3 mm has been widely studied, but only few reports were found on condensation heat transfer inside vertically oriented channels even for channel diameters greater than 3 mm. Condensation heat transfer inside extruded aluminium tubes and enhanced tubes are seen as emerging technologies. Considerable reports of applying heat transfer correlations to smaller diameter channels; however, those correlations were recommended and also derived with larger diameter channels are reported in the literature. A single general correlation to predict accurately the condensation heat transfer can still not be found even for larger diameter channels. However, several correlations are found which are valid in certain given ranges and under certain conditions. Condensation heat transfer for small diameter channels is still at the investigation level and no correlation has still been generally accepted as reliable.

2.3 Summary of the nine publications

2.3.1 Paper I: Charge Distribution in a 5 kW Heat Pump using Propane as Working Fluid, Part I: Experimental Investigation

This paper was prepared in order to find the answers to the question "How is the refrigerant distributed within the refrigerant circuit of the heat pump?"

An experimental setup mimicking a heating-only, liquid-to-liquid heat pump was constructed using brazed plate heat exchangers as evaporator and condenser, a scroll compressor and a thermostatic expansion valve. Four pneumatically operated ball valves were connected between the evaporator and compressor, between the compressor and condenser, between the condenser and expansion valve and between the expansion valve and evaporator, respectively (see Fig. 2.5). Propane was used as working fluid of the heat pump. Heat for evaporation was supplied by an electrically heated glycol solution which was circulated in a secondary closed loop. The condenser was cooled by water circulating in a secondary closed loop. This loop was cooled by a cold water tank.

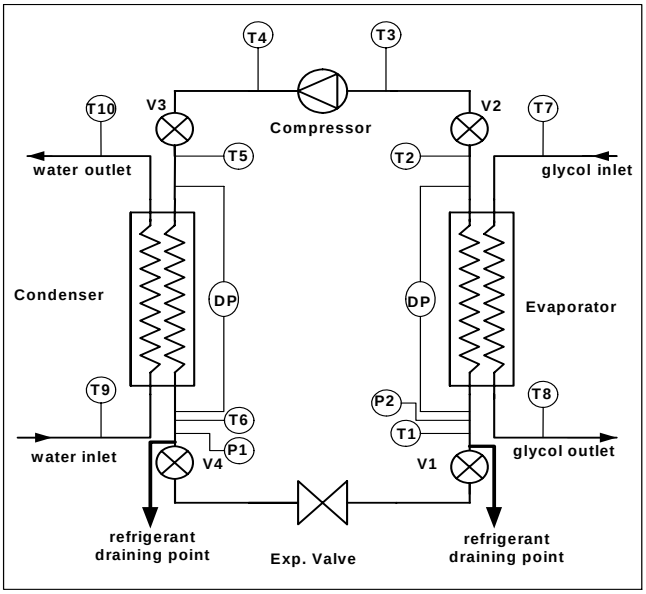

Fig. 2.5. Schematic diagram of the test facility.

The following conditions were maintained in the heat pump during the tests: The secondary refrigerant (glycol) inlet temperature of the evaporator was maintained between around -1°C to -3°C and the secondary fluid

(water) outlet temperature of the condenser was maintained between around 39°C to 40°C. While maintaining these conditions, the refrigerant charge in the heat pump was incremented stepwise from an initial charge barely large enough for the system to operate. After each increment of the refrigerant charge, and when the system had stabilized, measurements were taken of the evaporation temperature, condensing temperature, pressure drops, heat flows and input power to the compressor. After each such measurement, the heat pump was stopped by simultaneously closing the four ball valves in order to trap the refrigerant quantities inside the various sections of the refrigerant circuit. Then the refrigerant quantities located in each of the sections was drained separately into a cylinder and weighed. Variations in refrigerant hold-up in the evaporator, condenser, liquid line and compressor are shown in Fig. 2.6. The largest amount of the refrigerant charge was found in the condenser (Con-g), second in the evaporator (Eva-g), third in the compressor that included gas line (Gas-g) and finally the lowest amount in the liquid line that included expansion valve (Liq-g). The refrigerant amounts in the compressor and evaporator were almost independent of the total refrigerant charge. The refrigerant amount in the liquid line increased with increased total refrigerant charge up to 280 g and thereafter it was unchanged. The refrigerant amount in the condenser began to increase rapidly after total refrigerant charge reach to about 290 g.

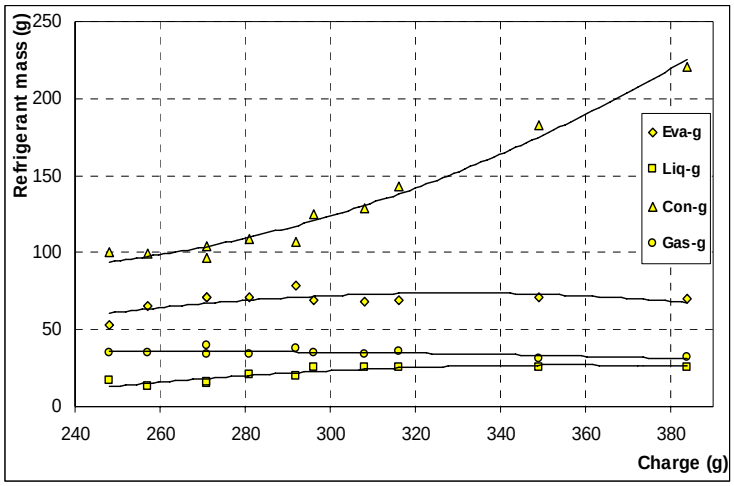

Fig. 2.6. Variations of refrigerant hold-up in various sections of the test-rig with refrigerant charge.

Variation in the coefficients of performance (COP) for various refrigerant charges is shown in Fig. 2.7. At lower refrigerant charges (below 280 g), refrigerant vapour bubbles passing through the expansion valve and

higher refrigerant superheating at the evaporator outlet results in reducing the COP. At higher refrigerant charges (above 320 g), condensing pressure increasing due to accumulation of additional refrigerant in the condenser results in decrease in the COP. As shown, the optimum refrigerant charge, i.e. the refrigerant charge giving the highest COP, was found between 280 - 320g at the investigated running conditions. The refrigerant amounts in the different components under these conditions were found to be as follows: In the evaporator 70 - 80 g, condenser 100 - 130 g, liquid line 26g and compressor 35 -40 g (Fig. 2.6). In these measurements, 35 - 40g of propane was missing (undrained) and could not be accounted for. It was believed that the missing quantity was dissolved in the compressor lubrication oil and could therefore not easily be evacuated from the system. Later, this assumption was confirmed by allowing several hours for evacuation and by stirring the oil by starting the compressor for a short moment during the evacuation period.

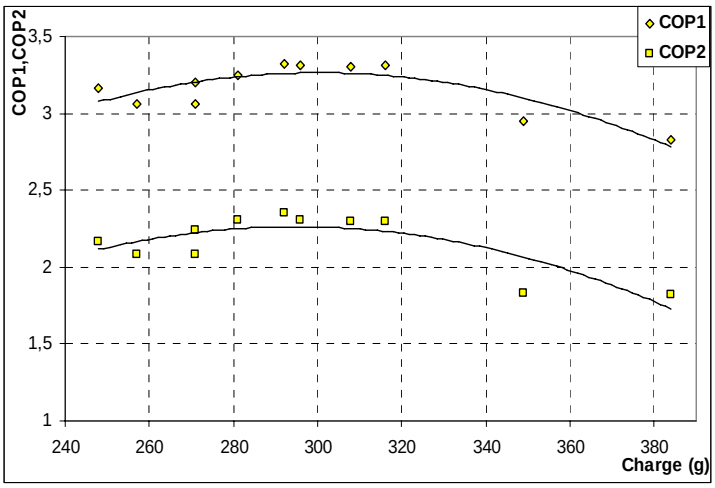

Fig. 2.7. Variations in COPs with the refrigerant charge.

The following decisions were made after these experiments,

a. To replace the brazed-plate heat exchangers with minichannel heat exchangers having smaller internal volumes compared to the tested brazed-plate heat exchangers.
b. To investigate the solubility of propane in different types of compressor lubrication oils.

2.3.2 Paper II: The Behaviour of Small Capacity (5 kW) Heat pump With Micro-Channelled Flat Tube Heat Exchanger

This paper was prepared in order to find the answers to the question "Can the refrigerant charge be reduced by introducing minichannel heat exchangers?"

In a second phase of the project, the brazed plate type heat exchangers (evaporator and condenser) of system described in *Paper I* was replaced by microchannel-flat-tube heat exchangers. These heat exchangers were constructed from flattened copper tubes having an internal cross sectional area of 0.6×6.3 mm^2 and the hydraulic diameter of 1.096 mm. The length of each tube was 400 mm. A heat exchanger unit was constructed by connecting 60 tubes in parallel to one inlet and one outlet plenum. The tubes were arranged in two rows, each consisting of 30 tubes. These heat exchanger units were commercially available and installed in most *Thermia heat pumps* several years ago. However, the production has now been ended and the heat exchangers substituted for brazed plate heat exchangers in *Thermia's* products.

Four such heat exchanger units were found in our laboratory and considered suitable for the project due to their small internal volumes. An evaporator was constructed by connecting two of these heat exchanger units in parallel and a shell was built to facilitate the secondary refrigerant fluid flow. A condenser was constructed by connecting two of these heat exchangers in series and as for the evaporator a shell was made for the cooling water flow.

In the following tests the condenser capacity and the coefficient of performance (COP) of the heat pump was determined for various refrigerant charges. Tests were run with the evaporation temperature fixed at -16°C, -8°C, 0°C and +5°C. The cooling water outlet temperature of the condenser was fixed between 39°C to 40°C for all four cases. The optimum refrigerant charge of the heat pump was determined for each case in the way described above (*Paper I*). Variation in COP1 with refrigerant charge for the above evaporation temperatures are shown in Fig. 2.8.

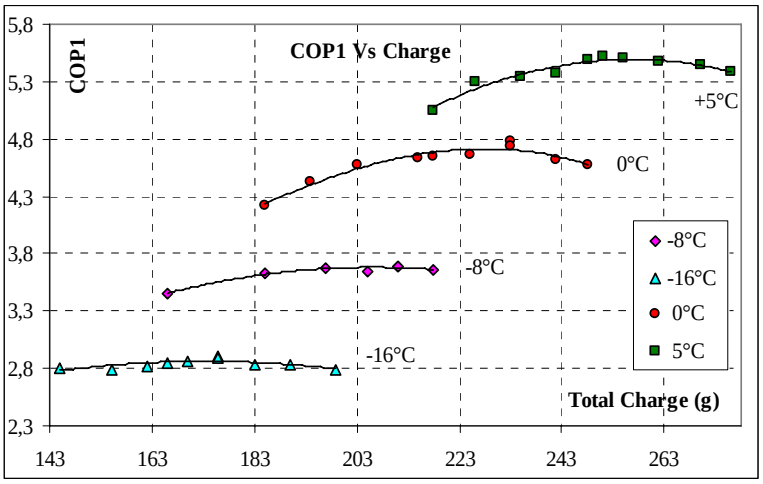

Fig. 2.8 Variation in coefficient of performance (COP1) with the total amount of refrigerant charge in the test-rig at evaporation temperatures -16°C, -8°C, 0°C & +5°C with a constant condenser cooling water outlet temperature (39-40 °C).

The optimum refrigerant charges at evaporation temperatures of -16°C, -8°C, 0°C and +5°C were between 170 - 180 g, 195 - 205 g, 225 - 235 g and 250 - 260 g, respectively, as shown in Fig. 2.8. The refrigerant amounts in various sections for a total refrigerant charge close to above optimum charges are presented in Table 2.4.

Table 2.4. Refrigerant amounts in different components at various evaporation temperatures with a constant condensing temperature.

Evaporation temperature (°C)	-15.9	-8.1	-0.2	4.9
Condensing temperature (°C)	41.1	40.8	41.1	40.8
Heat sink temperature (°C)	38.5	37.9	37.9	37.5
Heat source temperature (°C)	-3.9	6.0	14.5	20.5
Total refrigerant charge (g)	186	215	239	256
Amount in evaporator (g)	31	32	34	32
Amount in condenser (g)	77	83	78	72
Amount in liquid line (g)	20	18	21	25
Amount in gas line & compressor (g)	34	64	84	103
Amount in additional lines Provided for pressure measurements (g)	8	10	11	11
Amount of undrained (g)	16	8	15	27

Several interesting conclusions can be drawn from the results that displayed in Table 2.4 and Fig. 2.83. It is obvious from Table 2.4 that the necessary amount of refrigerant increases with increasing evaporation temperature. However, the amounts in the heat exchangers and in the liquid line are more or less constant. The amount in the discharge line

together compressor, on the other hand, increases substantially and corresponds exactly to the total increase in charge when the evaporation temperature is increased from -15.9 to 4.9°C. Two explanations to this increase of refrigerant in the compressor can be given: First, with increasing evaporation temperature, the vapour pressure and the vapour density will increase. The compressor has a fairly large internal volume and with increasing pressure and density the additional mass necessary to fill up this volume may correspond to a substantial part of the measured increase. Second, the increase in pressure may also increase the solubility of propane in the compressor oil so that more propane is absorbed in the oil. Note that the amount of undrained refrigerant in the data reported in *Paper I* was 35 -40 g. The amount of undrained refrigerant has been dramatically reduced in this report due to the fact that the refrigerant in the compressor was drained several times. After each draining, the compressor was either heated up by an electric heater or left several hours to boil-off the refrigerant that was dissolved in the oil. Therefore, it was very clear that the undrained refrigerant in *Paper I* was in the compressor.

For the purpose of comparison, a test was conducted with similar test conditions as those used with brazed-plate-heat exchangers. Switching from brazed-plate heat exchangers to flat-tube-minichannel heat exchangers resulted in a reduction of the total refrigerant charge from 292 to 215 g at the evaporation temperature of -8°C. The amount of refrigerant in the evaporator was reduced from 79 to 32 g and the amount in the condenser was reduced from 107 to 83 g. In the compressor the amounts were approximately the same for both cases, as could be expected.

The logarithmic mean temperature differences (LMTD) between propane and the secondary refrigerants of the evaporator as well as of the condenser were higher with the flat-tube-minichannel heat exchangers than with the brazed-plate heat exchangers. Therefore, the overall heat transfer coefficients of the flat-tube-minichannel heat exchangers were less than those of the brazed-plate heat exchangers. This was mainly due to the smaller heat transfer areas of the flat-tube-minichannel heat exchangers compared to the heat transfer areas of the brazed-plate heat exchangers. Note that the heat source and heat sink temperatures of the heat pump with brazed plate heat exchangers were -2.04°C and 39.72°C, respectively and for the heat pump with minichannel heat exchangers 5.98°C and 37.88°C, respectively. But evaporating and condensing temperatures of the heat pump with the brazed plate exchangers and with minichannel heat exchangers were almost same.

The following decisions were made after these experiments.

a. To construct a minichannel evaporator and a minichannel condenser having similar heat transfer areas as the previously tested brazed-plate heat exchangers (*Paper I*).
b. To further investigate the solubility of propane in oil.

2.3.3 Paper III: The Solubility of Propane (R290) with Commonly Used Compressor Lubrication Oil

This paper was prepared in order to find the answer to the question "Is it possible to reduce the refrigerant charge by changing compressor lubrication oil?"

First, this paper presents an analysis of the amounts of refrigerant inside the hermetic scroll compressor (and the discharge-line) from the measurements reported in the previous tests. Note that the undrained refrigerant reported in the previous tests was assumed to be in the compressor. By measuring the internal volumes of the suction-side and discharge-side of the compressor, it was possible to determine the amount of propane in vapour phase in the compressor at different pressures and temperatures. By knowing the total (measured) amount of propane, the amount dissolved in the compressor oil could be determined for the tested evaporation temperatures (at -16°C, -8°C, 0°C and 5°C) and condensing temperature (+40°C). The measured refrigerant amount in the compressor, calculated amount in the oil, calculated amount in the suction-side-free-space and calculated amount in the discharge-side-free-space are shown in Fig. 2.9.

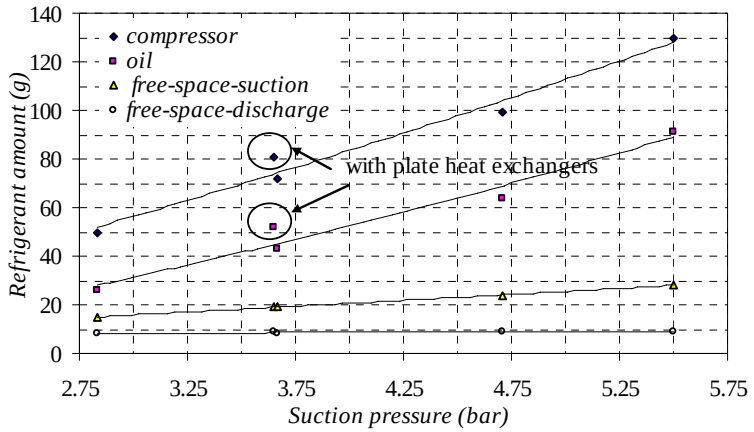

Fig. 2.9. Variations in refrigerant amounts in different parts of the compressor as a function of compressor suction pressure.

Note that the refrigerant charge distribution for the heat pump with plate heat exchangers was conducted at only one evaporation pressure and the circled data points represent the data with plate heat exchangers. They were a little higher, probably due to a possible experimental error.

With this increase of the evaporation temperature, the total mass of refrigerant in the compressor increased from 50 to 130 g. The amount of refrigerant in the free-space of the compressor suction-side was calculated to increase from 15 to 28 g and the mass of refrigerant on the compressor discharge side was constant about 8 - 9 g. From these values, the mass of refrigerant dissolved in the lubrication oil was estimated to increase from 26 to 91 g with the increase of the evaporation temperature (see Fig 2.9). The total amount of refrigerant on the compressor suction-side (in oil and free-space) varied from 41 to 119 g. Since the compressor contained 1.2 l of ester type oil, the ratio between propane/oil in the suctions side was increased from 3 to 10%.

Second, this paper presents results from solubility tests of propane with various types of lubricating oils. In these tests, different proportions of propane and oils were mixed in a glass tube. The glass tube was attached to a special arrangement connected to a motor rocking mechanism. The experiments were conducted in a controlled environment (in a temperature controlled chamber). The chamber was provided a heating/cooling facility in order to vary the temperature of the chamber. A picture of the test-facility is shown in Fig. 2.10.

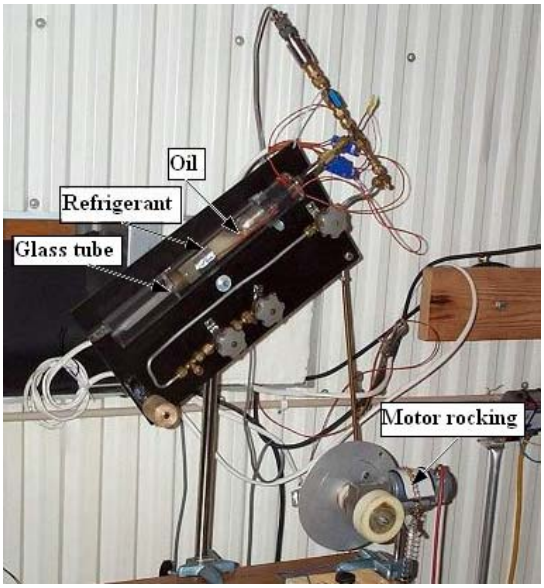

Fig. 2.10. A picture of the test facility.

The temperature of the chamber was varied while rocking the glass tube. The vapour pressures and temperatures of the propane-refrigerant mixtures were recorded.

Three different types of compressor lubrication oils were used: Two synthetic ester (POE) based oils (CPI EXP-2028 and RL32CF) and one polyalkylene glycol (PAG) based oil (CPI-1507-32). The vapour pressures of refrigerant-oil solutions are always less than the vapour pressure of the pure refrigerant [17]. As a result of the solubilities of refrigerants, the lubricating fluid can no longer be treated as a pure lubricant. The amount of refrigerant dissolved in a lubricant depends on the pressure and the temperature [17]. The vapour pressure of a refrigerant-lubricant mixture is equal to the sum of partial pressures of individual components. Generally, partial pressures of refrigerant lubricants at moderate temperatures are very small. Therefore, the vapour pressure of the mixture is very close to the vapour pressure of the refrigerant. In these tests, separation of liquid refrigerant and oil was visible before attaching the tube to the rocking mechanism. The mixtures were prepared at room temperatures (at about 25°C). The vapour pressure of the mixture should be close to the saturation pressure of the propane. As a result of high solubility, larger deviations of vapour pressure curves of the mixtures from the saturation pressure curve of the propane could be expected. The tests showed higher deviations of vapour pressure curves of the POE (polyol ester) oil than of PAG (polyalkylene glycol) oil, indicating higher solubility of propane in POE oils than in PAG oils. The tests also showed higher deviations when oil contents in the mixtures were increased. As mention before, the propane/oil ratio of the compressor suction side (by mass) was less than 10% for all tests. The vapour pressures for mixtures of 10% propane and 90% oils vs. the temperature are shown in Fig. 2.11. The two POE oil mixtures have almost identical vapour pressure curves, considerably lower than for pure propane, while the curve of the PAG-oil deviates much less from that of the pure propane.

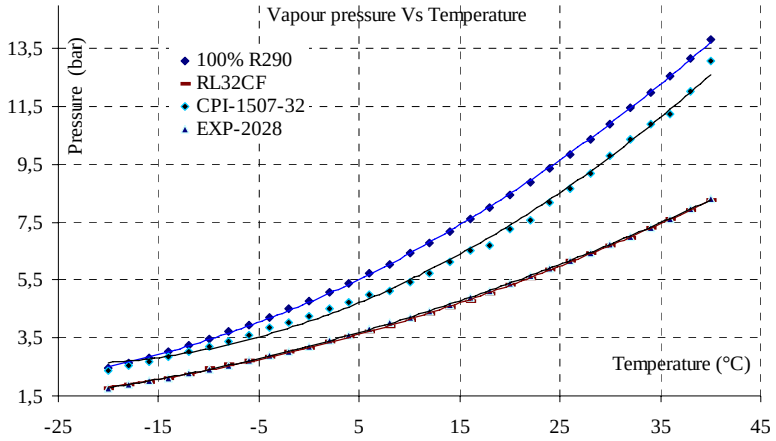

Fig. 2.11. Vapour pressure variation in 10% propane (90% oil) mixture and 100% propane at different temperatures.

The following conclusions were drawn after these experiments,

a. The mass of lubrication oil in the compressor should be kept at the minimum amount required for proper lubrication of the compressor.
b. The tested PAG type lubrication oil is better compared with POE type lubrication oils in concern of charge minimisation.
c. Tests should be done replacing the existing POE type oil in the compressor with PAG type oils to investigate the system performance with this oil. The compatibility of PAG oils with the compressor materials should be checked before tests.
d. Further studies should be done regarding compressor lubrication oils.
e. Other types of compressors requiring less oil should be sought and tested.

2.3.4 Paper IV: Minichannel Aluminium Heat Exchangers with Small Inside Volumes

This paper was prepared in order to find the answers to the question "Is it possible to design more compact heat exchangers than those available in the market and how the performance of the newly designed heat exchangers compared to those is available on the market?"

Paper IV first describes the design and manufacturing procedures of the minichannel heat exchangers. Second, correlations used for pressure drop calculations of the evaporator and for calculation of overall heat transfer coefficients are presented. It also presents the measured performance of the heat pump connected to the minichannel aluminium

heat exchangers at four different evaporation temperatures with a constant condensing temperature. Finally, a comparison of brazed plate and minichannel aluminium heat exchangers as evaporator and condenser are presented.

Three heat exchangers were constructed using multiport minichannel aluminium tubes. The evaporator and condenser of the previously described experimental setup (described in *Papers I and II*) were replaced by two of these heat exchangers. This paper compares the heat transfer performances of the multiport-minichannel-aluminium heat exchangers with those of the previously tested brazed-plate heat exchangers that was reported in *Paper I* connected to the same test-rig.

The new heat exchangers were designed as shell-and-tube heat exchangers, with refrigerant passing through the rectangular channels of the flat multiport aluminium tubes and secondary refrigerant passing in the shell, in narrow slots formed in between the tubes. The heat exchanger used as evaporator was constructed using 30 multiport extruded aluminium tubes and the heat exchanger used as condenser was made from 36 multiport extruded aluminium tubes. A picture of a tube cross section is shown in Fig. 2.12. A detailed cross sectional drawing of the aluminium tube is shown in Fig. 2.13. Each tube consisted of six channels. The four middle channels were equal in size: 1 mm in height and 2.65 mm in width. The two channels at the edges were 1 mm in height with a width of 1.45 mm plus a semi-circular part with a radius of 0.5 mm. The wall thickness of the tube was 0.5 mm. The hydraulic diameter ($4A_{cross}/p_t$) of a tube was 1.42 mm. The cross sectional area (A_{cross}) and wetted perimeter of a tube (p_t) were taken as the total of all six channels when calculating the hydraulic diameter.

The tubes, each with the length 661 mm, were arranged in two rows (15 tubes in a row for the evaporator and 18 in a row for the condenser) and held in place by 31 equally spaced (c/c approximately 19 mm) 1 mm thick aluminium baffle plates. The ends of the tubes were fixed to two aluminium end plates. The thickness of an end plate for the evaporator was 5 mm and for the condenser was 8 mm. The tube bundle was placed inside a shell made from four aluminium plates. Grooves were milled in the shell plates to hold the baffle plates in position. The whole unit was brazed together at the connecting points. A picture of a brazed unit is shown in Fig. 2.14a. Each baffle plate was joined to three shell plates and a 4.5 mm gap was left to the fourth plate. Ports were added at the ends of the heat exchanger to serve as inlet and outlet ports for the shell-side fluid. Pyramid shaped end-caps were attached to the two end plates, acting as inlet and outlet distributors for the tube-side fluid. A picture of an end cap is shown in Fig. 2.14 b. The active heat transfer areas on the

tube-side and shell-side of the evaporator were approximately 0.78 m^2 and 0.82 m^2, respectively. The active heat transfer areas of the tube-side and the shell-side of the condenser were 0.941 m^2 and 0.985 m^2, respectively. The total length of a heat exchanger was approximately 700 mm. A picture of a designed heat exchanger is shown in Fig. 2.15.

Fig. 2.12. End view of multiport extruded aluminium tube.

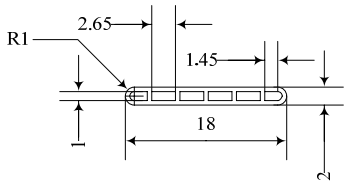

Fig. 2.13. Cross sectional drawing of a tube (all dimensions are in mm).

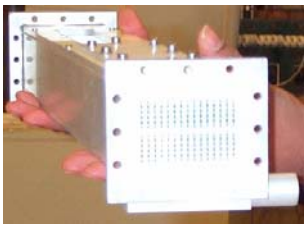

(a) Brazed unit.

(b) End cap.

Fig. 2.14. A picture of a brazed unit and a picture of an end cap.

Fig. 2.15. A picture of a heat exchanger.

The evaporator and condenser were vertically mounted. An externally-heated glycol solution entered through the upper port of the evaporator

shell travelled a serpentine path defined by the baffle plates, and left via the lower port. Propane with a desired inlet vapour quality flowed upward through the tubes and exited with a few degrees of superheat. The propane vapour from the compressor entered and exited the condenser tubes through the top and bottom end caps, respectively. The secondary fluid (water) entered the shell via the lower side port, travelled a serpentine path defined by the baffle plates, and exited from the upper side port.

The required evaporator and condenser capacities are approximately 3.75 kW and 5 kW respectively, when the system operates at a heat source temperature of -2°C and a heat sink temperature of +40°C. Tests were done first to determine the charge of refrigerant giving the highest COP of the system at the conditions at which the system was run with brazed plate heat exchangers (heat source temperature -2°C, heat sink temperature +40°C). Comparison of experimental results of the brazed-plate-type heat exchangers and minichannel heat exchangers with this optimum charge are presented in Table 2.5 and 2.6.

Table 2.5. Comparison of heat exchangers as an evaporator.

Duty requirements and physical parameters		Brazed plate evaporator		Aluminium evaporator	
		Side 1	Side 2	Side 1	Side 2
Fluid name		Propane	Eth. glycol	Propane	Eth. glycol
Liquid concentration	%		41.02		38.17
Evaporation temperature	°C	-9.73		-8.74	
Superheat	K	7.42		6.12	
Inlet temperature	°C	-9.16	-1.98	-7.82	-1.96
Outlet temperature	°C	-2.31	-5.15	-2.62	-5.27
Pressure drop	kPa	6.5		10.88	
Total heat of rejection	kW	3.58		3.86	
Mass flow rate-total	kgs^{-1}	0.013	0.334	0.013	0.337
Total heat transfer area	m^2	0.88	0.88	0.78	0.82
LMTD	K	5.29		4.18	
Overall H.T.C	$Wm^{-2}.K^{-1}$	770		1145	
Number of channels		7	8	180	
Fluid hold-up volume	cm^3	800	900	356.5	1277
Total number of plates/tubes		16		30	
Length	mm	67		84	
Width	mm	117		96	
Height	mm	524		721 (including in/out connections)	
Refrigerant hold-up	g	69		28	
COP2		2.31		2.70	

Table 2.6. Comparison of heat exchangers as a condenser.

Duty requirements and physical parameters	Brazed plate condenser		Aluminium condenser	
	Side 1	Side 2	Side 1	Side 2
Fluid name	Propane	Water	Propane	Water
Condensing temperature °C	42.42		39.50	
Sub cooling K	10.4		5.69	
Inlet gas temperature °C	78.01	31.92	67.64	31.86
Outlet temperature °C	31.93	39.82	33.73	39.61
Pressure drop kPa	2.12		2.26	
Total heat rejection kW	5.16		5.14	
Mass flow rate-total kgs^{-1}	0.013	0.156	0.013	0.158
Total heat transfer area m^2	1.01	1.01	0.94	0.98
LMTD K	5.69		3.61	
Overall H.T.C $Wm^{-2}.K^{-1}$	897		1456	
Number of channels	14	15	216	
Fluid hold-up volume cm^3	900	900	428.2	1520
Total number of Plates/tubes	30		36	
Length mm	98		84	
Width mm	72		108	
Height mm	465		721(including in/out connections)	
Refrigerant hold-up g	125		96	
COP1	3.32		3.59	

A comparison of braze plate and minichannel aluminium heat exchangers as evaporators is shown in Table 2.5. The heat transfer areas of the minichannel and plate-type heat exchangers were approximately equal. As shown, the volume of the refrigerant side of the minichannel aluminium evaporator was 356.5 cm^3 as compared to 800 cm^3 for the brazed plate evaporator. The logarithmic mean temperature difference (LMTD) between the refrigerant (propane) and the secondary refrigerant (glycol) at these conditions was 5.29K for the brazed-plate evaporator and 4.18K for the minichannel aluminium evaporator. This corresponds to an overall heat transfer coefficient for the plate-type evaporator of 770 $Wm^{-2}K^{-1}$ and of 1145 $Wm^{-2}K^{-1}$ for the minichannel aluminium evaporator (about 50% increases). The refrigerant content in each of the components was measured as previously described using the quick-closing valves. The mass of propane in the minichannel evaporator was 28 g and in the brazed-plate evaporator 69 g. The COP2 of the system using the minichannel heat exchangers as evaporator and condenser was increased from 2.31 to 2.70. These values are based on the heat flows and temperatures measured on the secondary side of the evaporator and compressor power measured by an electricity meter. The pressure drop of the refrigerant side of the minichannel aluminium evaporator was increased by about 50% compared to the brazed plate heat exchanger, but was still well within acceptable limits (about 11 kPa, gives about 0.9 K temperature drop in these operating conditions).

For the condensers, the volume was reduced from 900 to 428 cm^3. The LMTD between the refrigerant and water was 5.69 K for the brazed-plate condenser and 3.61 K for the minichannel aluminium condenser. This corresponds to an overall heat transfer coefficient for the brazed-plate condenser of 897 $Wm^{-2}K^{-1}$ and of 1456 $Wm^{-2}K^{-1}$ for the minichannel aluminium condenser (more than 60% increase). The refrigerant content in the minichannel condenser was 96 g and in the brazed-plate condenser was 125 g. The COP1 of the system using the minichannel heat exchangers as evaporator and condenser was increased from 3.32 to 3.59. These values are based on the heat flows measured on the secondary side of the condenser and compressor power measured by an electricity meter. The pressure drops of the condensers were both very low and more or less identical (2.2 kPa).

Paper IV also reports on tests with the minichannel heat exchangers at four different evaporation temperatures (-15.9, -8.3, -0.3 and +4.9°C) and a condensing temperature of +41°C. The results clearly demonstrate the good performances of the new heat exchangers for all these conditions, with LMTDs in the evaporator ranging from 3.4 to 5.0 K and in the condenser from 2.6 to 5.9K.

The following conclusions were drawn after these experiments,

a. Minichannel aluminium heat exchangers dramatically reduce refrigerant charge in heat pumps and refrigeration systems.
b. These heat exchangers not only minimise the refrigerant charge, they also give higher overall heat transfer coefficients that leads to better performance (higher COPs) of the system.
c. For better prediction of the performance of the new type of heat exchangers more detailed heat transfer data is needed. It was therefore decided to investigate single-phase heat transfer coefficients of both the shell and tube-side, evaporative heat transfer coefficients of the tube-side and condensation heat transfer coefficients of the tube-side of the minichannel aluminium heat exchangers.

2.3.5 Paper V: A Minichannel Aluminium Tube Heat Exchanger - Part I: Evaluation of Single-Phase Heat Transfer Coefficients by the Wilson Plot Method

This paper was prepared in order to find the answers to the question "Are the available correlations for single-phase heat transfer from the literature valid for the newly designed heat exchanger?"

To allow correct calculation of the refrigerant-side heat transfer, one of the aluminium heat exchangers was tested with water both on the shell-side and inside the tubes. This was done primarily in order to determine the single-phase heat transfer coefficient on the shell-side, as knowledge of the shell-side heat transfer is necessary to determine the boiling and condensation heat transfer coefficients from measurements of the overall heat transfer coefficients. In this paper these single-phase tests are reported.

As already noted, the heat exchanger was made from extruded multiport aluminium tubes and was designed similar to a shell-and-tube type heat exchanger. The heat exchanger tested for single-phase heat transfer was similar to the minichannel evaporator reported in the *Paper IV*. The only difference between those two heat exchangers was the thickness of the end palates. An end plate of the evaporator was 8 mm thick and of the heat exchanger tested for single-phase was 5 mm. Therefore, the effective heat transfer length of the evaporator tubes was little lower than the other. Heat transfer areas of the shell and tube-sides were approximately 0.82 m^2 and 0.78 m^2, respectively. There were six rectangular shaped parallel channels in each tube. The hydraulic diameter of the tube-side was 1.42 mm and of the shell-side 3.62 mm. More details of the design were given above in Table 2.5 in section 2.4.4.

Tests were conducted with varying water flow rates, temperature levels and heat fluxes on both the tube and shell-side. The Reynolds numbers for the tube-side were in the range $170 < Re < 6000$ and for the shell-side $1000 < Re < 5000$.

The Wilson plot method was employed to investigate heat transfer on the tube-side of the heat exchanger: While keeping the flow on the shell-side constant, the flow on the tube-side was varied corresponding to the Reynolds number range $2300 < Re < 6000$. The inverse of the measured overall heat transfer coefficients were plotted versus the inverse of the volume flows to the power of an unknown exponent n (initially assumed as 0.8). Then the value of n was determined as the value which resulted in a linear relationship. This value was found to be 1.25. The following correlation for the Nusselt number was found to represent the experimental data with good accuracy,

$$Nu = 4.526 \times 10^{-4}\ Re^{1.25}\ Pr^{0.4}\left(\frac{\mu}{\mu_s}\right)^{0.14} \tag{2.3}$$

The experimental data for this range of Reynolds numbers was also compared to several correlations from the literature suggested for turbulent or transition flow. The experimental and predicted Nusselt numbers

were area averaged and are shown as a function of *Re* in Fig. 2.16. It was found that the experimentally determined Nusselt numbers of the tube-side agreed with the Gnielinski [66] correlation within ±5 % .

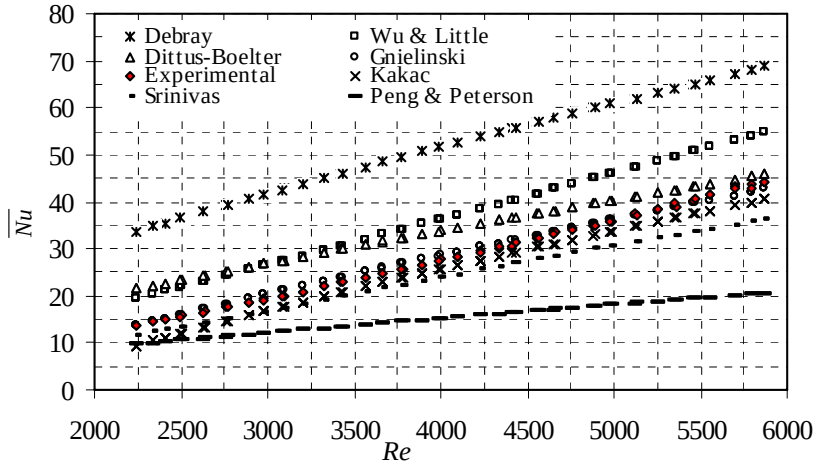

Fig. 2.16. Comparison of the average Nusselt number with correlations proposed for the turbulent and transition regimes from the literature.

The variation in *Nu* with *Re* for laminar flow (*Re* < *2300*) from the tests and from the correlations is shown in Fig. 2.17. None of the correlations predicted the Nusselt numbers well in this range of Reynolds numbers.

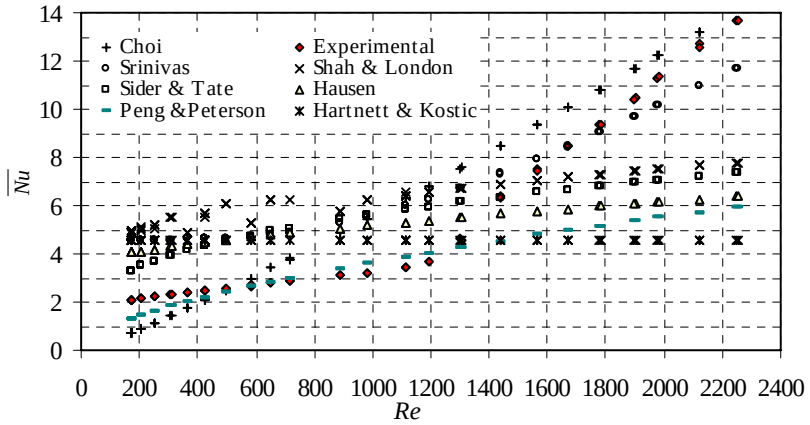

Fig. 2.17. Comparison of experimental Nusselt numbers with predictions from the literature for *Re* < *2300*.

The hydrodynamic entry length for laminar flow in a tube is obtained from the expression [67],

$$\frac{x_{fd,h}}{d_h} \approx 0.05Re \tag{2.4}$$

The thermal entry length for laminar flow in a tube is obtained from [68],

$$\frac{x_{fd,t}}{d_h} \approx 0.05Re\,Pr \tag{2.5}$$

The average Prandtl numbers of the above tests were in the range 5.30 - 6.60. The hydrodynamic entry length calculated by Eq. (2.4) was 160 mm at Re = 2250 and the thermal entry length calculated by Eq. (2.5) was 850 mm at the same Reynolds number. Since the effective length of a heat exchanger tube was 651 mm, a thermally fully developed flow did not occur even at the outlet of the tube at higher Reynolds numbers. At the lowest tested Reynolds number, 170, the hydrodynamic and thermal entry lengths were 12 mm and 80 mm, respectively. At Re = 800, the calculated thermal entry length was approximately half of the entire tube length. In conclusion, it is reasonable to expect the average Nusselt numbers to increase gradually with the Reynolds number as entrance effects become increasingly important. In the range $170 < Re < 1200$ the Nusselt number gradually increased with increasing Reynolds numbers from Nu = 2.1 to 3.7 (see Figure 2.17). This is, however, lower than predictions from correlations. Possible reasons could be maldistribution, which may be caused by the inlet velocity of the water into the header or axial conduction.

Tests were also conducted with varying flows on the shell-side. These tests were done to determine the influence of the Reynolds number on the shell-side Nusselt number. To allow determination of local Nusselt numbers, shell-side water temperatures were measured at 15 locations (including inlet and outlet) along the flow and based on these measurements the heat transferred in each of the 14 sections was determined. From these values, local Reynolds and Prandtl numbers were determined. Shell-side heat transfer coefficients were determined, using the heat transfer coefficient predicted by the Gnielinski [66] correlation for the tube-side. Finally, average values of Re, Pr and Nu were determined for the full length of the heat exchanger from the corresponding local values. The variation in the ratio of average Nu to $Pr^{0.4}$ as a function of Re is shown in Fig. 2.18.

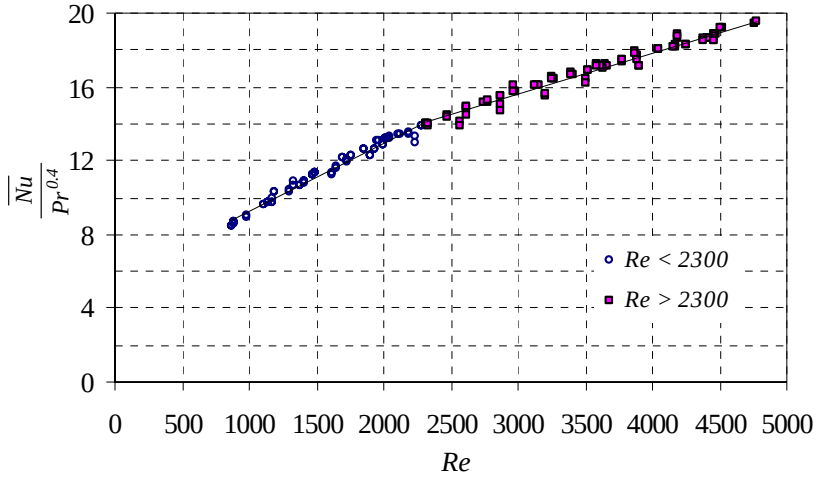

Fig. 2.18. Ratio of average Nu to $Pr^{0.4}$ as a function of Re.

A slight change in the inclination of the curve was found at Re = 2300, and two correlations are therefore suggested for the Nusselt number. The predictions of these correlations deviate less than 5% from the experimentally determined values in the Reynolds number range 1000 < Re < 4700.

For Re < 2300,

$$\overline{Nu} = (0.0037\,Re + 5.532)\,Pr^{0.4} \tag{2.6}$$

For Re > 2300,

$$\overline{Nu} = (0.0022\,Re + 8.859)\,Pr^{0.4} \tag{2.7}$$

The shell-side Nusselt numbers were also compared to correlations from the literature. None of the tested correlations could predict the experimental data, which was found to be considerably higher than predicted by correlations from the literature. An important reason for this may be the turbulence generated at the constrictions of the flow at the passage of each baffle plate.

The following conclusions were drawn after these experiments.

a. Two correlations for heat transfer were proposed for two Reynolds number ranges of single-phase flow on the shell-side of the minichannel aluminium heat exchanger.

b. A correlation was proposed to predict single-phase heat transfer on the tube-side of the minichannel aluminium heat exchanger for *Re* > *2300*.
c. The Gnielinski [66] correlation was found to predicted heat transfer on the tube-side of the minichannel aluminium heat exchanger very well for *Re* > *2300*.

2.3.6 Paper VI: A Minichannel Aluminium Tube Heat Exchanger - Part II: Evaporator Performance with Propane

This paper was prepared in order to find the answer to the question "Are the available correlations for evaporative heat transfer from the literature valid for the narrow channels of the newly designed heat exchanger?"

This paper presents heat transfer data for a multiport minichannel heat exchanger tested as a vertically mounted evaporator in the previously described experimental setup mimicking a liquid-to-liquid heat pump. The heat exchanger tested here as an evaporator is the same one used as evaporator in the tests described in section 2.4.4 and almost similar to that tested in single phase flow in the previous section (*Paper V*). The details of the design were given above in Table 2.5.

In the tests, propane entered the bottom end of the tubes with a desired vapour quality, flowed upward through the tubes and exited with a desired superheat of 1 K to 4 K. A temperature-controlled glycol solution that flowed downward on the shell-side supplied the heat for the evaporation of the propane. The heat transfer rate between the glycol solution and the propane was controlled by varying the electric power heating the glycol solution. As the compressor speed was kept constant, an increase of the electric power resulted in an increase of the evaporation temperature and thereby in an increase in the propane mass flow rate. The glycol flow rate was fixed at 18.50 $lmin^{-1}$. Tests were conducted for a range of evaporation temperatures from -15 to +10°C, corresponding to heat flux from 2000 to 9000 Wm^{-2} and mass flux from 13 to 66 $kgm^{-2}s^{-1}$.

Four series of tests were conducted. In the first three, the evaporation temperature was allowed to float with the supplied heat load to the evaporator. The difference between these series was the condensing temperature, being 30, 40 and 50°C, respectively. As the sub-cooling was just a couple of degrees in each case, the condensing temperature directly influenced the vapour fraction at the inlet of the evaporator. In the fourth test series, the evaporation temperature was kept constant at +10°C and the condensing temperature at +45°C. The refrigerant mass flow varied by adjusting a valve in the suction line before the compres-

sor. In each test series, tests were done with the superheat setting at 1, 2, 3 and 4K.

The evaporator was evaluated in 11 sections defined by the 12 temperature measurement locations along the glycol flow path. Each section could be considered as a small heat exchanger with the measured glycol temperatures as inlet and outlet temperatures. A temperature distribution of the two fluids for a typical case is shown in Fig. 2.19.

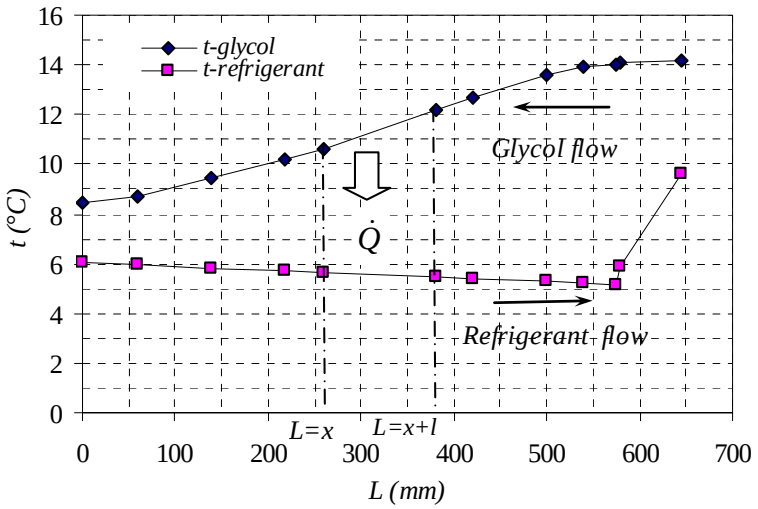

Fig. 2.19. Typical temperature distributions of the two fluids along the evaporator.

The refrigerant temperature was measured only at the inlet and outlet. The local temperatures were calculated from the local saturation pressures, which were estimated from the measured inlet pressure and measured total pressure drop, assuming a linear pressure drop from the inlet to outlet. For each of the sections, the local overall heat transfer coefficients were calculated based on the local logarithmic mean temperature difference. To find the boiling heat transfer coefficients inside the tubes, the shell-side heat transfer coefficients were first calculated according to Eq. (2.6). The boiling heat transfer coefficients of each section were then calculated from the relation,

$$\frac{1}{UA} = \frac{1}{\alpha_1 A_1} + \frac{\delta_t}{k_t A_m} + \frac{1}{\alpha_2 \left(A_b + \xi A_f \right)} \tag{2.8}$$

Finally, the average boiling heat transfer coefficients of the entire tube length were calculated as an area-weighted average of the local values of each section.

The results from Test Series 1, 2 and 3 were very similar, indicating that the inlet vapour quality had very little effect on the boiling heat transfer (since they were quiet close). The superheat at the evaporator exit had a clear, but limited effect on the heat transfer coefficients, with the values for 1K superheat being 400 to 700 $Wm^{-2}K^{-1}$ higher than those for 4K superheat (see Fig. 2.20).

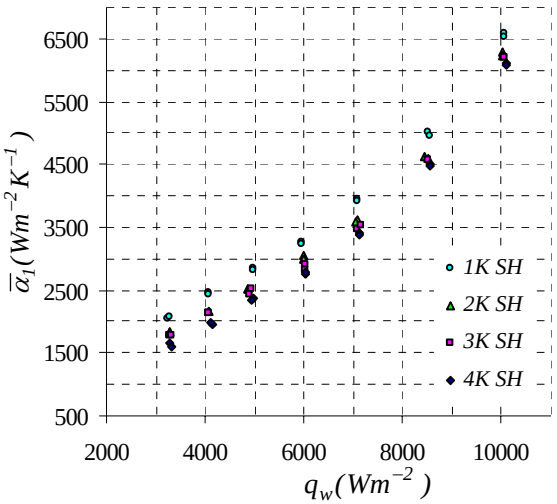

Fig. 2.20. Refrigerant-side average heat transfer coefficient vs. total heat flux in Test Series-2 {condensing temperature 40°C, evaporation temperature was increased from-15°C (q_w ≈3000 Wm^{-2}) to +15°C (q_w ≈10,000 Wm^{-2})}.

In all these tests, the heat transfer coefficient increased almost linearly with the heat load of the evaporator. It should be noted, though, that the heat load in these tests is directly connected to the mass flow and to the evaporation temperature.

In the fourth test series, in which the evaporation temperature was kept constant at +10°C, the heat transfer coefficients seem to level out at a value of 4000 to 4500 $Wm^{-2}K^{-1}$ (see Fig. 2.21).

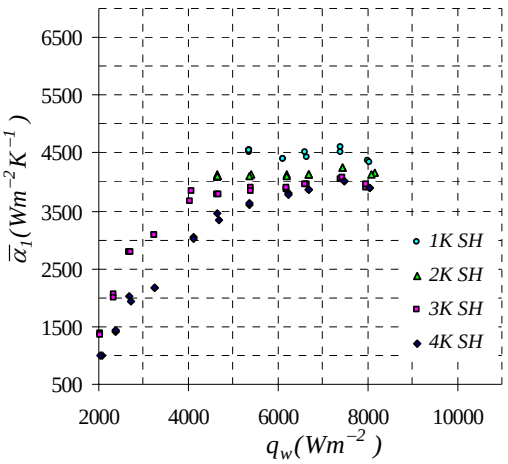

Fig. 2.21. Refrigerant side average heat transfer coefficient vs. total heat flux in Test Series- 4 (condensing temperature 45°C, evaporation temperature was +10°C).

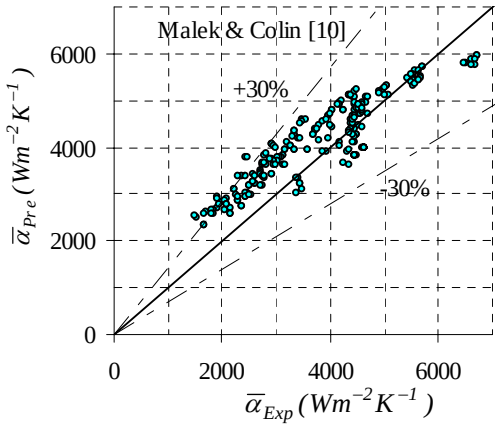

Fig. 2.22. Comparison of the experimental average heat transfer coefficient in the two-phase section with Malek & Colin [69] correlation.

The measured boiling heat transfer coefficients were compared with 14 correlations found in the literature. The experimentally determined heat transfer coefficients were in most cases higher than those predicted by the correlations. Still, most correlations seemed to catch the general trends of the experimental data, and by inserting a constant into some of the correlations the predictions of these could be made very much better. Malek and Colin correlation [69], which was developed for a very large and long tube (21 mm diameter and 10 m long), was in reasonable agree-

ment (95.56% data within $\pm 30\%$ deviation limit) with the experimental data (see Fig. 2.22).

In addition, Lazarek & Black [38], Kandlikar [30], Tran *et al.* [39, 70], Liu & Winterton [32] and Pierre correlations [71] were able to predict the data within a reasonable deviation (within $\pm 30\%$ deviation limit) after some adjustments in the correlations. Similarly, Cooper's pool boiling correlation [37] was in good agreement with the experimental data, if the predictions were multiplied by a factor of 1.5. Cooper [37] suggested scaling his original correlation by a factor of 1.7 (i.e., to change the constant 55 to 93.5) for horizontal copper cylinders. The scale factor was introduced to account for variations in tube geometry and material. By scaling Cooper's [37] original correlation by a factor of 1.7, 99.12% of the data were predicted within $\pm 30\%$ and 80.97% of the data were predicted within $\pm 20\%$.

The Lazarek & Black [38], Kandlikar [30], and Tran *et al.* [39, 70] correlations use the boiling number (*Bo*) to account for the contribution of nucleate boiling to the heat transfer coefficient. The Pierre [71] correlation uses Pierre's boiling number (K_f) to account for the contribution of nucleate boiling to the heat transfer coefficient. The Liu & Winterton [32] correlation uses the Cooper [37] nucleate pool boiling correlation for the contribution of nucleate boiling to the heat transfer coefficient. The Malek and Colin [69] correlation, which produced good agreement with the experiment heat transfer coefficients, is correlated with refrigerant mass flux, heat flux and reduced pressure. At smaller values of the boiling number, influence of the nucleate boiling is reduced and the dominant heat transfer mechanism is convective boiling. On the other hand, at higher boiling numbers the dominant heat transfer mechanism is nucleate boiling. Thus, the data comparisons indicate that the evaporative heat transfer process is strongly dominated by nucleate boiling.

The following conclusions were drawn from these experiments,

a. The experimentally determined heat transfer coefficients were in most cases higher than those predicted by the correlations from the literature.
b. Malek and Colin's [69] correlation was found to best predict heat transfer of the reported minichannel heat exchanger as evaporator.
c. Several other correlations would predict the heat transfer of the reported minichannel heat exchanger as evaporator much better, after inclusion of a constant.
d. Data comparisons indicate that the evaporative heat transfer process is strongly dominated by nucleate boiling.

2.3.7 Paper VII: A Minichannel Aluminium Tube Heat Exchanger - Part III: Condenser Performance with Propane

This paper was prepared in order to find the answer to the question "Are the available correlations for condensation heat transfer in the literature valid for the newly designed heat exchanger?"

This paper reports heat transfer data for condensation of refrigerant propane inside a minichannel aluminium heat exchanger mounted vertically as the condenser of the previously described heat pump system. The tested heat exchanger is the same one used as the condenser in the tests described in section 2.4.4. Propane vapour entered to the tube-side via the top end and liquid propane exited from the bottom end with a few degrees of sub-cooling. Coolant water entered the shell-side through a port provided on the lower end and left through a port provided on the upper end of the shell. The heat transfer areas of the tube-side and the shell-side were 0.941 m^2 and 0.985 m^2, respectively. The heat transfer rate between the two fluids was varied by varying the electric heating supplied to the glycol solution passing through the evaporator. Thereby, the evaporation temperature and the vapour density at the cold side changed, also changing the mass flow of refrigerant of the heat pump. The heat transfer rate between the two fluids was varied from 3900 to 9500 W. Experiments were conducted at constant condensing temperatures of 30°C, 40°C and 50°C, respectively. The cooling water flow rate was maintained at a constant value of 11.90 $lmin^{-1}$ for all tests. The test conditions are shown in Table 2.7.

Table 2. 7. Test conditions.

	Test Series -1	Test Series -2	Test Series -3
Water flow rate ($lmin^{-1}$)	11.90	11.90	11.90
Water-side *Pr*	5.37 - 7.33	4.25 - 5.82	3.52 - 4.54
Water-side *Re*	948 - 1255	1159 - 1528	1447 - 1820
Total heat transfer rate (W)	4155 - 8942	4045 - 9514	3992 - 9033
Refrigerant mass flux ($kgm^{-2}s^{-1}$)	20 - 47	20 – 53	19 - 52
Refrigerant inlet temperature (°C)	44 - 64	54 – 81	65 - 102
Condensing temperature (°C)	30	40	50
Sub-cooling (K)	2.4 - 3.94	2.23 - 3.71	2.59 - 3.60
Refrigerant-side vapour *Re*	3066 -7524	2800 - 8144	2539 - 7671
Refrigerant-side vapour *Pr*	0.81 - 0.86	0.82 - 0.88	0.82 - 0.90
Refrigerant-side liquid *Re*	310 - 729	337 - 908	364 - 1014
Refrigerant-side liquid *Pr*	2.85	2.83	2.83

As for the measurements on the evaporator, the condenser was evaluated in 14 sections defined by the 13 temperature measurement locations and two calculated temperature locations (at saturated conditions of the refrigerant) along the flow path. Each section could be considered as a

small heat exchanger with the measured water temperatures as inlet and outlet temperatures. A temperature distribution of the two fluids for a typical case is shown in Fig. 2.23.

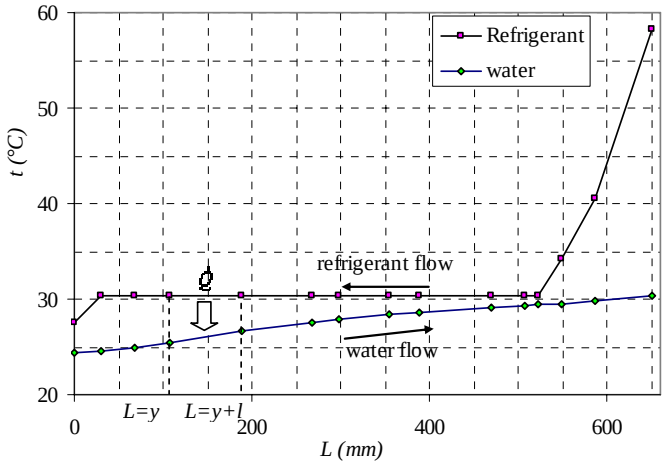

Fig. 2.23. Typical temperature distribution for the refrigerant and water flow along the condenser.

Note that the refrigerant side temperatures in the de-superheating and subcooling regions were calculated by heat balances between the water flow and the refrigerant flow. A detailed description of that is provided in *Paper VII*. The overall heat transfer coefficient of each section was calculated from the known heat load and the logarithmic mean temperature difference of the section. The shell-side heat transfer coefficient was calculated from Eq. (2.6), determined from the water to water tests described above. As for the evaporator, the refrigerant side heat transfer coefficient was then calculated from the overall and shell-side heat transfer coefficients using Eq. (2.8).

Lengths of the de-superheating, two-phase and sub-cooling sections were evaluated for all tests. The de-superheating, two-phase and sub-cooling lengths as a function of refrigerant mass flux for the condensing temperature 40°C is shown in Fig. 2.24. As shown, the sub-cooling section is always very short, and the length cannot be determined with high accuracy as it may be shorter than the length between the last two thermocouples. The length of the de-superheating section decreases with increased mass flux. This is because the inlet temperature of the gas from the compressor is higher at lower mass fluxes, as the lower mass fluxes were achieved by decreasing the evaporation temperature.

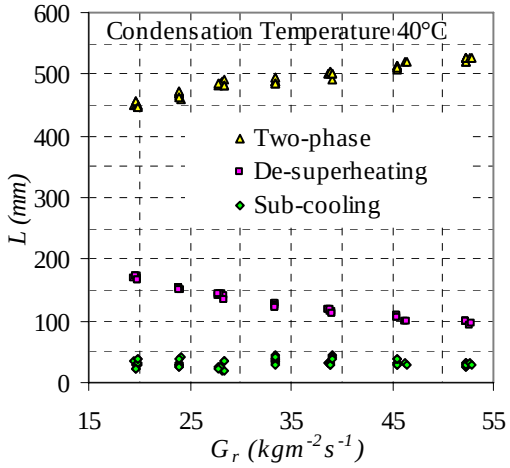

Fig. 2.24. Effect of refrigerant mass flux on two-phase, de-superheating and sub-cooling lengths for 40°C condensation temperature. {evaporation temperature was increased from-15°C (G_r ≈19 $kgm^{-2}s^{-1}$) to +15°C (G_r ≈53 $kgm^{-2}s^{-1}$ Wm^{-2})}.

The local heat transfer coefficients for each of the sections along the tube for the mass flux of 28 $kgm^{-2}s^{-1}$ are shown in Fig. 2.25.

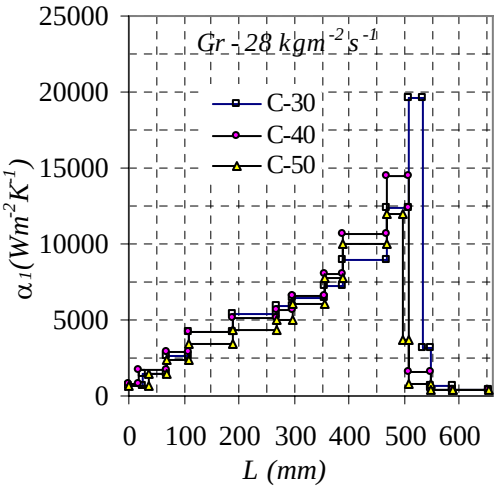

Fig. 2.25. Local heat transfer coefficient along the heat exchanger (from sub-cooling section to de-superheating section) for a mass flux of 28 $kgm^{-2}s^{-1}$ at different condensing temperatures.

The refrigerant enters from the right of the diagram. It is clear how the heat transfer coefficient increases to a peak value in the first part of the

two-phase region, and then decreases gradually as the liquid fraction increases towards the outlet. For each of the de-superheating, two-phase and sub-cooling sections, the area-averaged heat transfer coefficients were also calculated. Some of these heat transfer coefficients, determined from the measurements with 40°C condensing temperature, are shown in Fig. 2.26.

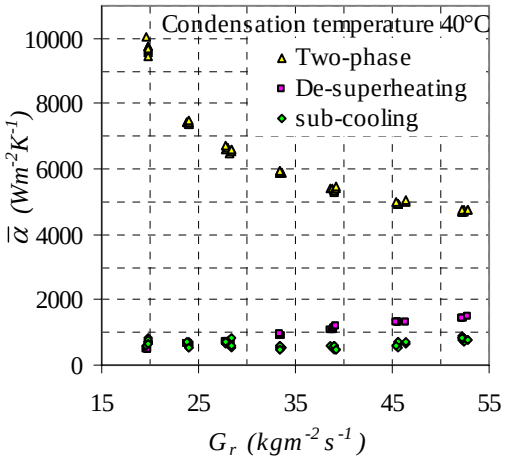

Fig. 2.26. Effect of mass flux on average heat transfer coefficient in the different regions for 40°C condensation temperature.

The experimentally determined average heat transfer coefficients of the three sections were also compared to correlations suggested in the literature. For the de-superheating section, only the first part was used, where the wall temperature was above the saturation temperature of the fluid. As this section is quite short, the flow may not have been fully developed. This may explain why the heat transfer coefficients were higher than expected from most of the correlations used for the comparison.

The heat transfer coefficients in the condensing section of the tubes were compared to several correlations from the literature for condensation inside tubes. None of the correlations accurately predicted the experimental heat transfer coefficients of the two-phase section. Chato [73], Nusselt [74], and Kutateladze [75] correlations underpredicted the experimental two-phase heat transfer coefficients. However, all followed the trend, indicating gravity dominated heat transfer mechanism. Those three correlations were modified by multiplication by a constant factor related to the mean deviation of the respective correlations. After this, the correlations were able to predict the experimental heat transfer coefficients within ±15% . Of those modified correlations, the modified Nusselt [74] correlation was giving better predictions than the other two. The reason for the under prediction of the Nusselt theory is probably

that the surface tension forces act to draw the liquid to the corners of the rectangular channels, thereby decreasing the film thickness on part of the surface.

The heat transfer coefficients of the sub-cooling section were much higher than expected, probably due to uncertainties caused by the small temperature differences. Also, the length of this section could not be determined exactly.

The following conclusions were drawn from these experiments,

a. Heat transfer coefficients in de-superheating and sub-cooling sections were compared with single-phase correlations from the literature and were found to be under predicted by the correlations.
b. Heat transfer coefficients in the two-phase section were also higher than those predicted by correlations from the literature.
c. Chato [73], Nusselt [74], and Kutateladze [75] correlations were easily modified to fit the heat transfer data within an accuracy limit of $\pm 15\%$.

2.3.8 Paper VIII: Propane Heat Pump with Low Refrigerant Charge: Design and Laboratory Tests

This paper was prepared in order to find the answers to the question "What is the optimum refrigerant charge of the heat pump with the newly designed heat exchangers? How is the performance of the heat pump at the optimum charge with the newly designed heat exchangers?"

In the reported tests in *Paper VIII*, the condenser capacity and the coefficient of performance (COP) of the heat pump was determined for various refrigerant charges. Tests were conducted with the heat source temperature fixed at -10°C, -2°C, +6°C and +12°C. The cooling water inlet and outlet temperatures of the condenser were fixed at 33°C and 40°C, respectively, for all four cases. The optimum refrigerant charge of the heat pump was determined for each case in the way described in *Paper I*. Variation in COP1 with refrigerant charge for the above conditions is shown in Fig. 2.27.

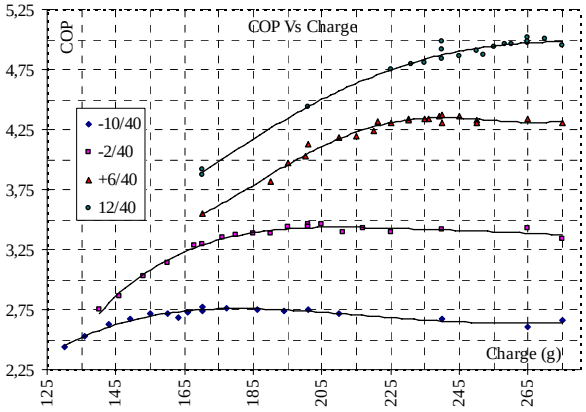

Fig. 2.27. COP1 of the heat pump vs. refrigerant charge for four heat source temperatures (-10°C, -2°C, 6°C, 12°C) at a constant heat sink temperature 40°C.

The optimum refrigerant charges at heat source temperatures (-10°C, -2°C, 6°C, 12°C) were about 170 g, 200 g, 240 g and 265 g, respectively, as shown in Fig. 2.27. The refrigerant charge distributions in the various sections of the heat pump for optimum refrigerant charges are presented in Table 2.8.

Table 2.8. Refrigerant charge distribution in various components.

Heat source / Heat sink temperatures (°C)	-10.22 / 40.77	-2.09 / 40.67	6,93 / 40.77	12.64 / 40.74
Evaporation / Condensing temp. (°C)	-16.49 / 39.73	-8.79 / 40.44	-0.51 / 41.44	4.55 / 39.95
Evaporator / Condenser Capacity (kW)	2.67 / 4.00	3.66 /5.01	4.90 / 6.31	5.89 / 7.23
Super heat / Sub cool (K)	4.66 / 3.91	5.30 / 4.76	5.18 / 4.56	5.77 / 3.82
Optimum Refrigerant Charge (g)	170	201	240	265
Measured in Evaporator (g)	27	23	25	26
Measured in Condenser (g)	69	80	90	93
Measured in Liquid line (g)	24	24	23	24
Measured in Compressor (g)	50	74	102	122

The LMTD of the condenser was approximately 2.5, 3.25, 4 and 4.5 K at heat source temperatures of -10°C, -2°C, 6°C and 12°C, respectively, for their respective optimum charges. The LMTD of the evaporator was approximately 4, 4.25, 4.75 and 5 K at heat source temperatures -10°C, -2°C, 6°C and 12°C, respectively, for their respective optimum charges. The overall heat transfer coefficient of the condenser was increased approximately from 1500 to 1600 $Wm^{-2}K^{-1}$ with increased heat source temperature for optimum charge (Note that the LMTD was different for four conditions). The overall heat transfer coefficient of the evaporator

was increased approximately from 800 to 1400 $Wm^{-2}K^{-1}$ with increased heat source temperature for optimum charge.

According to Table 2.8, the amount of refrigerant in the evaporator was 23 - 27 g, condenser 69 - 93 g and compressor 50 to 122 g. Note that in these tests, the entire refrigerant charge in the heat pump was extracted (no missing refrigerant). To drain all the refrigerant in the compressor took about a day. According to Table 2.4, for the heat pump with flat tube minichannel heat exchangers, the amount of refrigerant in the evaporator was 31 - 34 g, condenser 72 - 83 g and compressor 50 - 130 g (missing amounts accounted to compressor). The refrigerant amounts in the minichannel aluminium heat exchangers and the minichannel flat tube heat exchangers were in the same range. However, the log mean temperature differences (LMTDs) in both minichannel aluminium evaporator and condenser were considerably lower than those of the minichannel flat tube heat exchangers. Therefore the overall heat transfer performances of the aluminium minichannel heat exchangers were considerably higher compared to the minichannel flat tube heat exchangers.

This paper also presents the performance of the heat pump charged with the above given four optimum charges and operating at different test conditions. For a fixed refrigerant charge (charged with a above optimum charge) and a fixed heat sink temperature (40°C), the heat source temperature was incremented from -12 to +12°C. COP1 of the heat pump was plotted against the heat source temperature for each load increment (see Fig. 2.28).

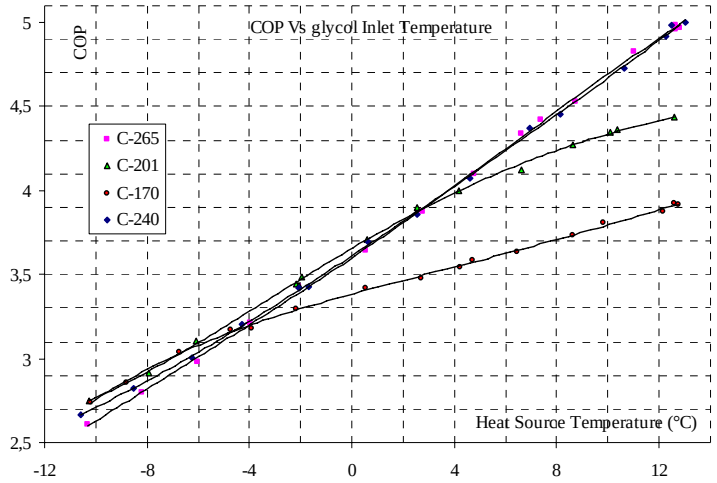

Fig. 2.28. Variations of COP1 with heat source temperature for four different refrigerant charges.

For heat source temperatures below -4°C, the refrigerant charge did not show a considerable influence on the COP1, however, the lowest system charge (170) gave the best performance. For heat source temperatures below 4°C, the refrigerant charge 201 g gave good performance but for heat source temperatures over 6°C the refrigerant charge 201 g was inadequate.

This paper also presents a set of ground temperature data measured during a heating season in Sweden. In addition, this paper also presents measured heat source temperatures (brine inlet temperatures) of a heat pump, (installed in Sweden) during the same heating season. The minimum brine inlet temperature of that season was -2.2°C and the COP1 of the heat pump reported in this paper at that heat source temperature was about 3.5 for the refrigerant charge 201g.

The following conclusions were drawn after these experiments.

a. Use of mini-channel heat exchangers reduces considerably the refrigerant charge in heat pumps and refrigeration systems.
b. The heat transfer coefficients of mini-channel heat exchangers are high, indicating that the reduction of charge can be reached without loss of COP.
c. Reduction of the tube lengths and exclusion of ball valves would give an optimum charge for the 5kW propane heat pump with ground heat source or other liquid-to-liquid type applications of less than 200g.
d. The proposed heat pump connected with ground source and a refrigerant charge of 200g would provide a minimum COP1 of 3.5.

2.3.9 Paper IX: Performance of a Single-Family Heat Pump at Different Working Conditions Using Small Quantity of Propane as Refrigerant

This paper was prepared in order to find the answers to the question "How is the performance of the heat pump with various heat source and heat sink temperatures connected to the newly designed heat exchangers?"

Our previous research work suggested that the optimum refrigerant charge increases with the increases of evaporation temperature (or heat source temperature) at a given condensing temperature. Too low or too high charge of a heat pump reduces the COP1. However, undercharge has a greater influence on the COP1 of the heat pump than over charge

(see Fig. 2.27). Generally, small heat pumps or refrigeration systems running with small refrigerant charges are designed without a receiver to hold up additional refrigerant that may be required in operating the heat pump at higher evaporation temperatures. Instead, the system could be charged with the minimum amount of refrigerant required to operate at its highest evaporation temperature. Alternatively it could be charged with the refrigerant amount giving the highest COP1 at its most frequent operating condition. However, these kind of systems are expected to operate in small evaporation (or heat source) temperature ranges.

Experiments were conducted charging the heat pump with the minimum amount of refrigerant required for a stable operation and without permitting refrigerant vapour escaping into the expansion valve, at a glycol (heat source) inlet temperature of +10°C. Then the glycol inlet temperature was varied from +10°C to -10°C while holding the condensing temperature constant. These tests were done with the condensing temperatures of 35°C, 40°C, 50°C and 60°C. The minimum refrigerant charges required for stable operations were found to decrease when the condensing temperature increased and were recorded as 230 g, 224 g, 215 g and 205 g, respectively. At high condensing temperatures, the length of the de-superheating section of the condenser could be expected to be larger than that at low condensing temperatures. The de-superheating section contains a relatively low amount of refrigerant as the refrigerant is in vapour phase. Therefore, increasing the size of the de-superheating section when increasing the condensing temperature should decreases the amount of refrigerant in the condenser.

The COP1 of the heat pump at the condensing temperatures 35°C, 40°C, 50°C and 60°C for the above refrigerant charges as function of heat source temperature is shown in Fig. 2.29. As expected, the COP of the heat pump was observed to be highly dependent on both the heat source and condensing temperatures.

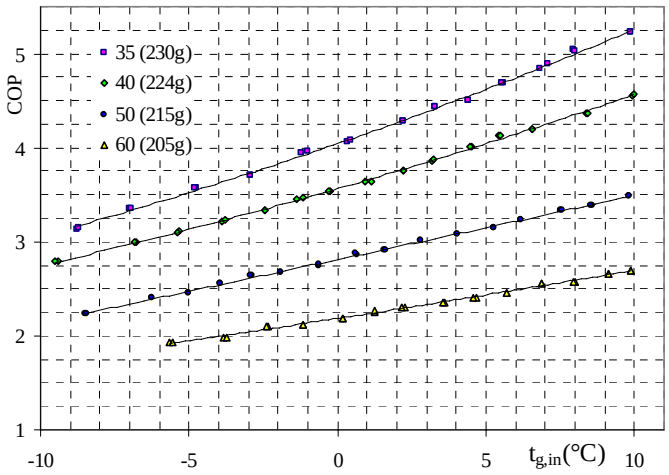

Fig. 2.29: Variations in COP1 of the heat pump with heat source temperature at different condensing temperatures.

This paper also present temperature data obtained from a ground source heat pump that was installed in a single-family house in Katrineholm, Sweden (170 km south-west of Stockholm). The design capacity of the heat pump system was about 5 kW. The system had a vertical ground loop collector in a 93 m deep borehole. A plastic U-tube with 40 mm inner diameter was used as the collector. The outdoor temperature and the temperatures of the borehole at different locations (25 m and 55 m) were measured from the spring of the year 2000 to the end of May 2002. The variations of hourly averaged outdoor temperature and temperatures in the borehole at given locations with time is shown in Fig. 2.30.

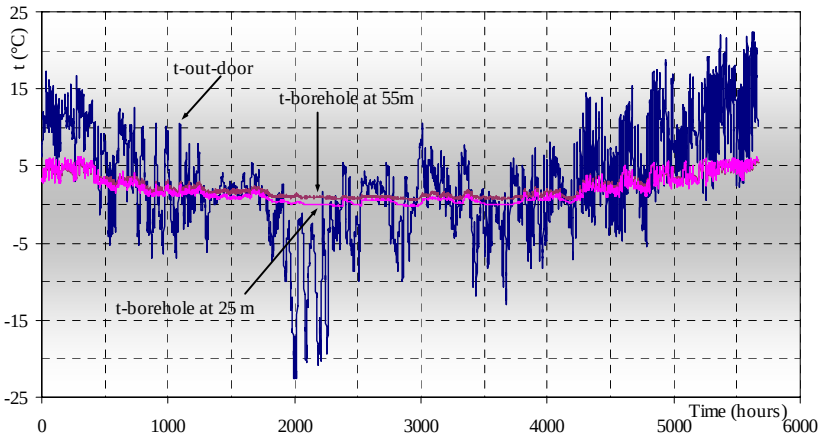

Fig. 2.30. Variations in the hourly averaged outdoor temperature, the temperature in the borehole at a depth of 55 m and at 25 m vs. time.

The measurements show that, although the outdoor temperature varied approximately 46°C during the measuring period, the temperature variation in both locations of the borehole was less than 7°C during the same period. The outdoor temperature was around zero or below zero for the time period from 1000 hrs to 4000 hrs thus representing the time period with the maximum heating demand of the house (see Fig. 2.30). The borehole temperature level during most of this period is considerably higher than the outdoor temperature level and also it was almost at a constant value. Since the evaporation temperature of a heat pump is related to the heat source temperature, the evaporation temperature variation in a ground source heat pump is much smaller than for an ambient air heat pump. The higher temperature level in the ground should therefore provide considerably higher COP with a ground source heat pump compared to an ambient air source heat pump.

The condensing temperature of a heat pump is related to the heat sink temperature (or supply temperature of the heating system). A high heat supply temperature to the house causes a high condensing temperature thereby increasing the compressor work which leads to a drop in the COP. Heat pumps with low-temperature heating systems such as low temperature radiators or floor-heating systems give excellent COPs. The typical heat supply temperatures for floor heating systems are about 35°C at design conditions. The main drawback of the low temperature heating systems is the requirement of lager radiators or floor heating resulting in higher investment costs [76]. The temperature range for low temperature radiators is 40°C to 45°C. Traditionally, buildings in Europe have heating systems designed for high water supply temperatures up to 80°C or 90°C with a temperature drop of 10°C to 20°C. Heat pumps are usually designed to provide hot water temperatures up to 50°C to 60°C with a temperature drop of 5°C to 6°C. The installation of heat pumps in existing traditional buildings thus requires complete replacement of the high temperature radiators with low temperature radiators [77].

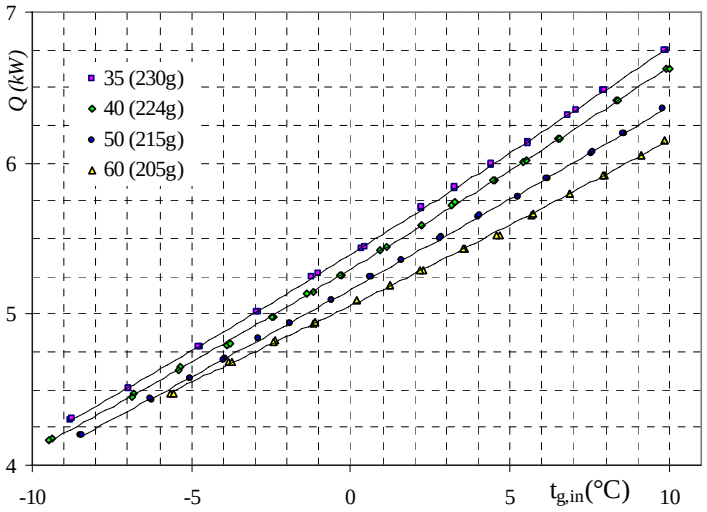

Fig. 2.31. Variations in heating capacity with heat source temperature at different condensing temperatures.

The capacity of the heat pump as a function of the heat source temperature is shown in Fig. 2.31. According to Fig. 2.30, the average bore-hole temperature was above 0°C. Therefore, use of ground source would be providing heating capacity above 5 kW (see Fig. 2.31) and minimum COP1 above 2.25 to 4 depending on the utilised heating system (see Fig. 2.29). For all cases, the refrigerant charge in the system was not more than 230 g. Note that, further reduction of the refrigerant charge (about 30 g) is possible by limiting the lengths of the connecting tubes. Therefore the final system charge would be about 200 g. Consideration of the solubility of propane in the lubrication oil suggest that the amount of refrigerant which may escape rapidly in case of an accident or leakage is probably less than 150g.

This paper also presents variation of compressor efficiency (hermetic efficiency, i.e. the isentropic efficiency calculated using the states of the refrigerant at the inlet and outlet of the shell of the hermetic compressor) as a function of pressure ratio for the tests conducted with the heat pump during the project (see Fig. 2.32). The scroll compressor used in these experiments was recommended for use with R407A and no data was available running with propane as refrigerant. However, this compressor was operated more than 5000 hrs with propane during the experimental period without considerable performance reduction.

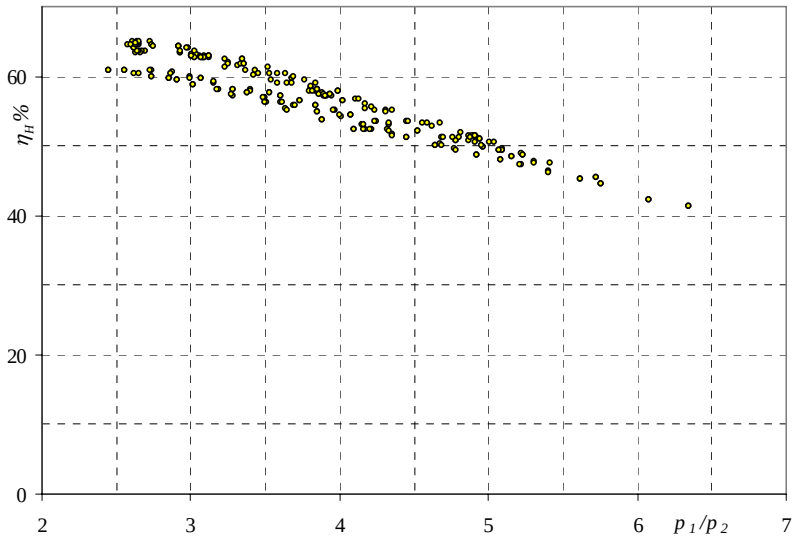

Fig. 2.32. Variation of the hermetic efficiency of the compressor with pressure ratio.

The following conclusions were drawn after these experiments,

a. The tested compressor is capable of operating with propane.
b. The ground is a better heat source option than air to achieve low charge of the heat pump as well as to obtain high COP levels as the evaporation temperature is higher and more stable during the heating season.
c. Increase of condensing temperature reduce the optimum refrigerant charge of the system but also reduce the COP.
d. Taking into account that some of the refrigerant is dissolved and bound in the compressor lubrication oil, the amount of rapidly escaping refrigerant in case of a accident or leak in the tested heat pump with minichannel heat exchangers would be less than 150g.

References

[1] Matrosv Yu.A., Butovsky I.N., Case studies of energy consumption in residential buildings in Russia's middle belt area, Energy and Buildings 20, 231-241, 1994.
[2] D. Chwieduk, Towards sustainable-energy buildings, *Applied Energy* 76, (1–3), pp. 211-217, 2003.
[3] Balaras C.A., K. Droutsa, E. Dascalaki, S. Kontoyiannidis, Heating energy consuption and resulting environmental impact of European apartment buildings, Energy and Buildings 37, pp. 129 - 442, 2005.

[4] Simonson C., Energy consumption and ventilation performance of a naturally ventilated ecological house in a cold climate, Energy and Buildings 37, 23-35, 2005.
[5] Olofsson T., Andersson S., Östin R., A method for predicting the annual building heating demand based on limited performance data, Energy and Buildings 28, 101-108, 1998.
[6] Forsén M., Lundqvist P., Field measurements on a single-family house in Sweden supplied with a ground source heat pump for heating and passive cooling. 4th int. conf., Heat pumps in cold climates Quebec 17-18 August 2000.
[7] Svensson H., Low energy consumption in Swedish single-family houses, Renewable Energy, Vol.5, Part II, pp. 997-999, 1994.
[8] C.A. Balaras, K. Droutsa, A.A. Argiriou and D.N. Asimakopoulos, Potential for energy conservation in apartment building, *Energy and Building* 31, pp. 143-154, 2000.
[9] P. Herant, Energy Situation and Energy Conservation Programme for Buildings in France, Energy Conservation in Buildings and Community Systems Programme, International Energy Agency, ECBCS News-Issue 34, pp. 1-6, October 2001.
[10] Sustainable energy policy to meet the needs of the future, Documentation 508, Federal Ministry of Economic and Technology, Berlin, (0342-9288), 2002, p. 121, June 2002.
[11] D. Lalas, C.A. Balaras, A. Gaglia, E. Georgakopoulou, S. Mirasgentis, I. Serafidis, S. Psomas, Evaluation of Supporting Policies for the Advancement of the Ministry's Policies in Relation to the Abatement of CO_2 Emissions in the Residential and Tertiary Sectors, IERSD, National Observatory of Athens, Ministry for the Environment Physical Planning and Public Works, Directorate Urban Planning and Housing, Athens 2002, p. 650 (in Hellenic).
[12] C.A. Roulet, Ecole Polytechnique Fidirale de Lausanne (EPFL), Lausanne, Switzerland.
[13] D. Chwieduk, Analysis of utilisation of renewable energies as heat sources for heat pumps in building sector in Poland, *Renewable Energy* 9 (1-4), pp. 720–723, 1996.
[14] J. Schnieders, CEPHEUS-Measurement Results from More Than 100 Dwelling Units in Passive Houses, ECEEE 2003 Summer Study-Time to Turn Down Energy Demand, St Raphael, France, pp. 341-351, June 2003.
[15] S.R. Hastings, Breaking the "heating barrier" learning from the first houses without conventional heating, *Energy & Buildings* 36 (4), pp. 373-380, 2004
[16] Bøhm B., P. O. Danig, Monitering the energy consumption in a district heated apartment building in Copenhagen, with specific interest in the thermodynamic performance, Energy and buildings 36 (3), 229 - 236, 2004.

[17] ASHRAE handbook, Refrigeration Systems and Applications, SI Edition, 1994, chapter 7. ISBN 1-883413-16-8
[18] Oliver Pelletier, "Propane as refrigerant in residential heat pumps", Engineering Licentiate thesis, Department of Energy Technology, Division of Applied Thermodynamics and Refrigeration, Royal Institute of Technology, Stockholm, Sweden, 1998, 15p
[19] Select Lubricants, PO Box 729, Montebello CA 90640-0729 USA, www.selectlubricants.com (2006-10-01)
[20] CPI Engineering Services, Inc., 2300 James Savage Blvd. Midland Ml 48642, www.cpieng.com, (2006-10-01)
[21] Guo Z.Y., X.B. Wu, Compressibility Effect on the Gas Flow and Heat Transfer in Micro Tube, Int. J. Heat Mass Transfer 40, P 3251-3254, 1997.
[22] Guo Z.Y., X.B. Wu, Further Study on Compressibility Effect on the Gas Flow and Heat Transfer in Microtube, Microscale Thermophys. Eng. 2, p111-120, 1998.
[23] Guo Z.Y., Z.X. Li, Size Effect on Microscale Single-Phase Flow and Heat Transfer, Int. J. Heat Mass Transfer 46, p149-159, 2003.
[24] M.J. Kohl, S.I. Abdel-Khalik, S.M. Jeter and D.L. Sadowski, An experimental investigation of microchannel flow with internal pressure measurements, *Int. J. Heat Mass Transfer* 48 (2005), pp. 1518–1533.
[25] R.K. Shah and A.L. London, Laminar flow forced convection in ducts: a source book for compact heat exchanger analytical data. , Academic Press, New York (1978) (Edited book)
[26] G.P. Celata, M. Cumo, V. Marconi, S.J. McPhail, G. Zummo, Microtube liquid single-phase heat transfer in laminar flow, *Int. J. Heat Mass Transfer*, 49 (2006), pp. 3538 - 3546.
[27] W. Zhang, T. Hibiki and K. Mishima, Correlation for flow boiling heat transfer in mini-channels, *Int. J. Heat Mass Transfer* 47 (2004), pp. 5749-5763.
[28] J.C. Chen, A correlation for boiling heat transfer to saturated fluid in convective flow, ASME Paper, 63-HT-34 (1963) 1-11.
[29] K.E. Gungor and R.H.S. Winterton, A general correlation for flow boiling in tubes and annuli. *Int. J. Heat Mass Transfer* 29, pp. 351-358, 1986.
[30] Kandlikar S.G., A general correlation for saturated two-phase flow boiling heat transfer inside horizontal and vertical tubes. Journal of Heat Transfer Transactions of ASME (112):pp.219-228, 1990.
[31] Steiner D., J. Taborek, 1992, Flow boiling heat transfer in vertical tubes correlated by an asymptotic model. Heat Transfer Engineering 13 (2), 43-69.
[32] Liu Z., W.H.S. Winterton, A general correlation for saturate and sub cooled flow boiling in tubes and annuli, base on a nucleate pool

boiling equation, International Journal of Heat and Mass transfer 34 (1991) 2759-2766.
[33] M.M. Shah, A new correlation for heat transfer during flow boiling through pipes, *ASHRAE Trans.* 82 (1976) (2), pp. 66-86.
[34] X. Boissieux, M.R. Heikal and R.A. Johns, Two-phase heat transfer coefficients of three HFC refrigerants inside a horizontal smooth tube. Part I. Evaporation, *Int J Refrigeration* 23 (2000), pp. 269-283.
[35] A. Koşar, C.J. Kuo and Y. Peles, Boiling heat transfer in rectangular microchannels with reentrant cavities, *Int. J. Heat Mass Transfer* 48 (2005) (23), pp. 4867-4886.
[36] D.S. Wen, Y. Yan and D.B.R. Kenning, Saturated flow boiling of water in a narrow channel: time-averaged heat transfer coefficient and correlations, *App. Therm. Eng.* 24 (2004), pp. 1207–1223.
[37] Cooper M.G., Heat flow rates in saturated nucleate pool boiling-A wide ranging examination using reduces properties. Adv. Heat transfer 16:157-239, 1984.
[38] Lazarek G.M, S.H. Black, Evaporative heat transfer, pressure drop and critical heat flux in a small vertical tube withR-113, International Journal of Heat and Mass Transfer 25(1982) 945-960.
[39] Tran T.N., M.W. Wambsganss , D.M. France, Small circular and rectangular-channel boiling with two refrigerants, International Journal of Multiphase flow, vol. 22, no. 3, pp. 485-498, 1996.
[40] Warrier G.R., V.K. Dhir, L.A. Momoda, Heat transfer and pressure drop in narrow rectangular channels, Exp. Thermal fluid sci. 26 (2002) 53-64.
[41] Kenning D.B.R., M.G. Cooper, Saturated flow boiling of water in vertical tubes, International journal of Heat and Mass Transfer 32 (1989) 445-458.
[42] T.Y. Choi, Y.J. Kim, M.S. Kim and S.T. Ro, Evaporation heat transfer of R-32, R-134a, R-32/134a, and R-32/125/134a inside a horizontal smooth tube, *Int. J. Heat Mass Transfer* 43 (2000), pp. 3651-3660.
[43] Gungor K.E., and R.H.S. Winterton, Simplified general correlation for saturated flow boiling and comparisons of correlations with data. *The Canadian Journal of Chemical Engineering, Chemical Engineering. Research & Design* 65, Issue 2 (1987), pp. 148-156.
[44] S. J. Eckels and M. B. Pate, An experimental comparison of evaporation and condensation heat transfer coefficients for HFC-134a and CFC-12 International Journal of Refrigeration, Volume 14, Issue 2, 1991, Pages 70-77, 1991.
[45] Shah M.M., A general correlation for heat transfer during film condensation inside pipes, Int. J. Heat Mass Transfer, Vol.22, pp 547-556, 1979.

[46] D.P. Traviss, W.M. Rohsenow and A.B. Baron, Forced convection condensation inside tubes: A heat transfer equation for condenser design. *ASHRAE Trans* 79 (1972), pp. 157-165.

[47] A. Cavallini and R. Zecchin, A dimensionless correlation for heat transfer in forced convection condensation. In: (Third Edition ed.), *Proceedings of the Fifth International Heat Transfer Conference Tokyo* Vol 3, pp. 309-313, 1974.

[48] Y.-Y. Yan and T.-F. Lin, Condensation heat transfer and pressure drop of refrigerant R134a in a small pipe, *Int. J. Heat Mass Transfer* 42, pp. 697-708, 1999.

[49] Y.S. Chang, M.S. Kim and S.T. Ro, Performance and heat transfer characteristics of hydrocarbon refrigerants in a heat pump system, *Int. J. Refrig.* 23, pp. 232-242, 2000.

[50] X. Boissieux, M.R. Heikal and R.A. Johns, Two-phase heat transfer coefficients of three HFC refrigerants inside a horizontal smooth tube. Part II. Condensation, *Int J Refrigeration* 23, pp. 345-352, 2000.

[51] M.K. Dobson and J.C. Chato, Condensation in smooth horizontal tubes. *ASME J. Heat Transfer* 120 (1998), pp. 193-213.

[52] Wang W-W.W., T.D. Radcliff, R. N. Christensen, A condensation heat transfer correlation for millimeter-scale tubing with flow regime transition, Experimental Thermal and Fluid Science, Vol. 26, Isssue 5, pp 473-485, 2002.

[53] Akers W.W., H.F. Rosson, Condensation inside a horizontal tube, Chem. Eng. Prog. Symp. Ser., Vol. 56, No. 30, pp. 145-149, 1960.

[54] Yang C. and R. Webb, Condensation of R12 in small hydraulic diameter extruded aluminium tubes with and without micro-fins. *Int. J. Heat Mass Transfer* 39, No**.** 4, pp. 791-800, 1996.

[55] Akers W.W., H.A. Deans, O.K. Crosser, Condensation heat transfer within horizontal tubes, Chem. Eng. Prog. Symp. Ser., Vol. 55, No. 29, pp. 171-176, 1959.

[56] Nae-Hyun Kim, Jin-Pyo Cho, Jung-Oh Kim and Baek Youn, Condensation heat transfer of R-22 and R-410A in flat aluminum multichannel tubes with or without micro-fins, *Int J Refrigeration* 26, *Issue 7*, pp. 830-839, 2003.

[57] R.L. Webb, Prediction of condensation and evaporation in microfin and micro-channel tubes. In: S. Kakac, A.E. Bergles, F. Mayinger and H. Yuncu, Editors, *Heat transfer enhancement of heat exchangers*, Kluwer Academic Publishers, Netherlands, pp. 529-550, 1998.

[58] Koyama S, Kuwahara K, Nakashita K, Yamamoto K. An experimental study on condensation of R134a in a multi-port extruded tube. In: Proceedings of 2002 International Refrigeration Conference at Purdue, R6-2, 2002.

[59] Koyama S., K. Kuwahara, K. Nakashita and K. Yamamoto, An experimental study on condensation of refrigerant R134a in a multiport extruded tube, *Int. J. Refrigeration* 26, pp. 425-432, 2003.

[60] K.W. Moser, R.L. Webb and B. Na, A new equivalent Reynolds number model for condensation in smooth tubes. *J. Heat Transfer*, 120, pp. 410–417, 1998.
[61] H. Haraguchi, S. Koyama and T. Fujii, Condensation of refrigerants HCFC22, HFC134a and HCFC123 in a horizontal smooth tube (2nd report, proposal of empirical expressions for the local heat transfer coefficient. *Trans. JSME (B)* 60, 574, pp. 245 - 252 [in Japanese], 1994.
[62] Mao-Yu Wen, Ching-Yen Ho and Jome-Ming Hsieh, Condensation heat transfer and pressure drop characteristics of R-290 (propane), R-600 (butane), and a mixture of R-290/R-600 in the serpentine small-tube bank, Applied Thermal Engineering, Vol. 26, Issue 16, pp. 2045 - 2053, 2006.
[63] Cavallini A., G. Censi, D. Del Col, L. Doretti, G.A. Longo, L. Rossetto and C. Zilio, Condensation inside and outside smooth and enhanced tubes: a review of recent research, *Int. J. Refrig.* 26 pp. 373-392, 2003.
[64] Ho-Saeng Lee, Jung-In Yoon, Jae-Dol Kim, P.K. Bansal, Condensing heat transfer and pressure drop characteristics of hydrocarbon refrigerants, *Int. J. Heat Mass Transfer* 49, Issue 11-12, pp. 1922–1927, 2006.
[65] J.S. Shin and M.K. Kim, An experimental study of condensation heat transfer inside a mini-channel with a new measurement technique, *International Journal of Multiphase Flow* 30, pp. 311-325, 2004.
[66] Gnielinski, V., *Int. Chem. Eng.*, 16, p. 359, 1976.
[67] Langhaar H.L., *J. Appl. Mech.*, 64, A-55, 1942.
[68] Kays, W.M., Trans. ASME, 77, p. 1265, 1955.
[69] Malek A., R. Colin, Ebullition de l'ammoniac en tube long. Transfert de chaleur et pertes de charges en tubes vertical et horizontal. Centre Technique des Industries Mecanniques, Senlis France, CETIM-14-011 1-65, 1983.
[70] Tran T.N., M.W. Wambsganss, D.M. France, Boiling heat transfer with three fluids in small circular and rectangular channels, Argonne National Laboratory, ANL-95/9 p.54, 1995.
[71] Pierre B., Värmeövergång vid kokande köldmedier i horisontella rör, Kylteknik tidskrift Vol.28, no.5, pp. 3-12 (Swedish), 1969.
[72] Cooper M.G., Heat flow rates in saturated nucleate pool boiling-A wide ranging examination using reduces properties. Adv. Heat transfer 16, pp.157-239, 1984.
[73] Chato J.C., "Laminar condensation inside horizontal and inclined tubes," *J.ASHRAE*, 4, 52, February 1962.
[74] Nusselt, W., 'Die Oberflächenkondensation des Wasserdampfes'. Zeitschr. Ver. Deutsch. Ing., 60, 541-569, 1916.
[75] Kutateladze, S.S., Fundamentals of heat transfer, Academic press, New York, 1963.

[76] Marcic M., long terms performance of central heat pumps in Slovenian homes, Energy and Building 36, 185 - 183, 2004.
[77] B. Sanner, C. Karystas, D. Mendrinos and L. Rybach, Current status of ground source heat pumps and underground thermal energy storage in Europe, *Geothermics* 32, pp. 579–588, 2003.

3 Measuring Instruments, Circuit Diagrams and Systematic Errors

Introduction

The test-facility was supplied with an electronic data acquisition system connected to a computer. This system included a junction box that allowed the connection of 58 thermocouples, 2 absolute pressure transducers, 2 differential pressure transducers and 2 magnetic flow meters. All measuring instruments were calibrated and tested against known values prior to using them in the experiments. The signals from the measuring instruments were read by two Agilent 34970A data loggers connected to a PC.

Generally, the errors that occur during a measuring period can be divided in to two categories: Systematic and random. Systematic errors are errors which tend to shift all measurements in a systematic way so their mean values are displaced. This may be due to incorrect calibration of equipment, consistently improper use of equipment or failure to properly account for some effects, etc. However, large systematic errors must be eliminated by good calibrations. But small systematic errors always are present. For instance, no instrument can ever be calibrated perfectly.

This section explains the measuring instruments used in the experiments, their electrical and electronic connections (circuit diagrams), calibrations and their systematic errors. The random errors will be discussed in the next section.

3.1 Temperature measurements

All temperature measurements in the test-rig were done using duplex insulated T type thermocouples. T type thermocouples have a positive copper wire and a negative constantan wire. The specifications of the thermocouple wires are shown in Table 3.1.

Table 3.1. Specifications of thermocouple wires.

Manufacturer	Omega engineering, INC.
ANSI colour code	Positive wire blue (Copper) / Negative wire red (Constantan)
Part number	TT-T-24-SLE
Lot number's	ICP12629P IHC012937P
Insp. Code	19638
Diameter of a wire	24 AWG (0.5106 mm)
Deviation	-0.1° F at 200° F

The thermocouples were connected to a junction box in which all the reference junctions (cold junctions) were placed inside an isothermal block, the temperature of which was measured by a Pt100 sensor. A circuit diagram of the thermocouples and the connection of the PT100 are shown in Fig. 3.1. Totally, 116 thermocouple wires were cut from the same main lot: 58 of them for the actual temperature measurements and the others (58) for use inside the junction box. The reference temperature block (isothermal block) was cut from an aluminium bar (approximately 5×5×10 cm^3), into which 59 holes were drilled on one of its sides (5×5 cm^2 side). The depths of the holes were just enough to pass the centre of the block (approximately 5 cm). About 5 mm of insulation at both ends of the thermocouple wires were removed and cleaned by a sand paper. In one of the ends the wires were twisted and brazed together (all 116). The other ends of 58 thermocouples that were prepared to be used as temperature sensors were connected to 58 connectors as shown in Fig. 3.1. The copper wires of the thermocouples were connected to the positive terminal of the connector and the constantan wires were connected to the negative terminal of the connector. All the connectors were labelled from 1 to 58. The same numbers were used for the thermocouples. For example, the thermocouple which was connected to the connector 1 was named as T1. The brazed ends of the thermocouples that were prepared to insert into the reference temperature block (other 58 thermocouples) were covered by small rubber capsules to avoid any electrical short circuit between thermocouples. The outer diameter of those rubber capsules was approximately similar to the diameter of the insulated thermocouple wires and the length was just enough to cover the brazed end of the thermocouple wires. The rubber capsules were then carefully heated to shrink them together with the thermocouples and then inserted into the 58 holes of the aluminium block. A 4-wire Pt100 sensor was carefully inserted to the middle hole of the aluminium block. The block was, then well insulated. The Pt100 had two white wires and two red wires. One red wire and one white wire were connected to the H terminal and the L terminal of CH1 of a HP 34901A 20-channel multiplexer, respectively, and the other two wires were connected to CH11 of the same multiplexer, feeding the sensor with the necessary current. CH1 of the multiplexer was used to measure

the reference temperature of the aluminium block. CH1 to CH20 of the 20-channel multiplexers are used to measure voltage signals and CH21 and CH22 are used to measure current signals. The positive terminals of the connector 1 was attached to the H terminal of the CH2 in the multiplexer and the L terminal of the same channel was connected to a copper wire of a thermocouple that was inserted to the aluminium block and the constantan wire of that thermocouple was connected to the negative terminal of the connector 1 as shown in Fig. 3.1. In the same way, all 58 connectors were connected to the three multiplexers. The 58 connectors were located at the top of the junction box and the insulated aluminium block was placed inside. The three modules of multiplexers were installed in the mainframe of an Agilent 34970A data logger. The data logger was connected to a computer. The software program HP VEE was used to read the measurements.

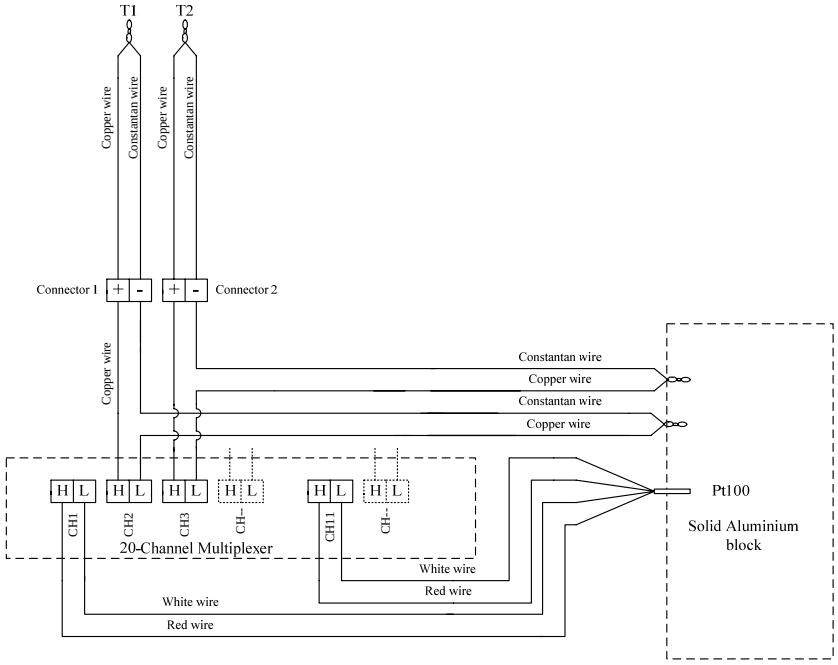

Fig. 3.1. Circuit diagram of thermocouple wires and connection of PT100.

3.1.1 Temperature calibration

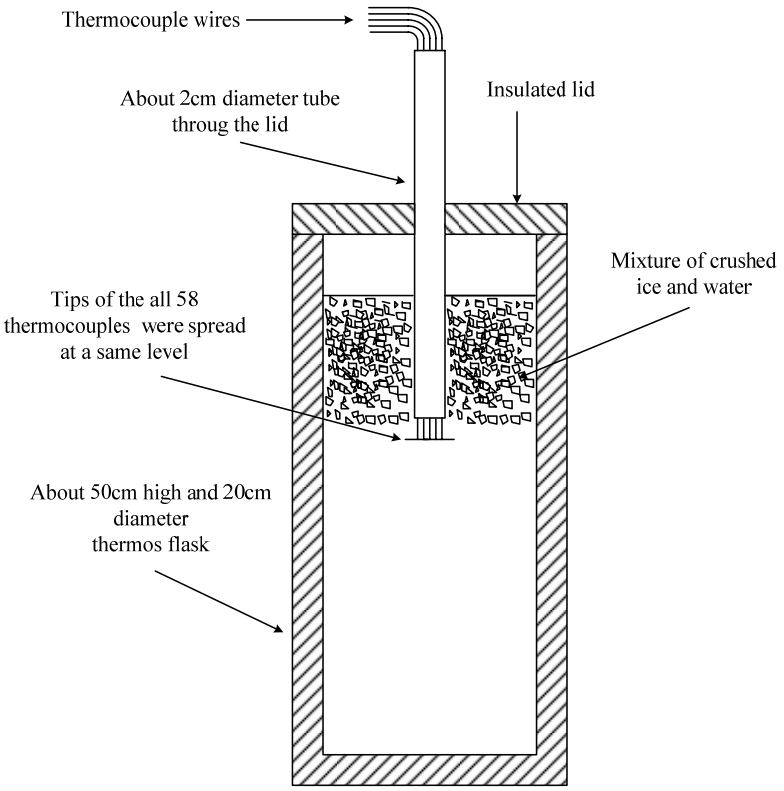

Fig. 3.2. The temperature calibration unit.

An ice bath was prepared in a thermos flask (assuming the temperature to be 0°C in the bath). The height of the thermos flask was about 50 cm and the diameter was about 20 cm. An about 2 cm diameter tube was fixed through the lid of the thermos flask. Crushed ice mixed with water filled the thermos flask up to about ¾ of its height. All the 58 thermocouples (prepared for temperature measurements) were inserted through the tube that was fixed to the lid of the thermos flask and the thermocouples were spread at a same height. The lid was adjusted in order to keep the tips of the thermocouples just below the ice-water level. The temperature calibration arrangement is shown in Fig. 3.2.

Temperature readings from the thermocouples were observed through the computer. Initially, the temperature readings were seen to be decreasing rapidly and then started to consolidate around 0°C. The arrangement was kept long enough (about 6 hours) to stabilise the temperature

around 0°C. The temperature readings of all 58 thermocouples were seen to deviate slightly from 0°C, however they were all at constant values. The temperature readings of the thermocouples were taken during a 15 minute period at 5 seconds intervals at stable a condition. Maximum, average and minimum temperature variations of all 58 thermocouples during the 15 minute period are shown in Fig. 3.3.

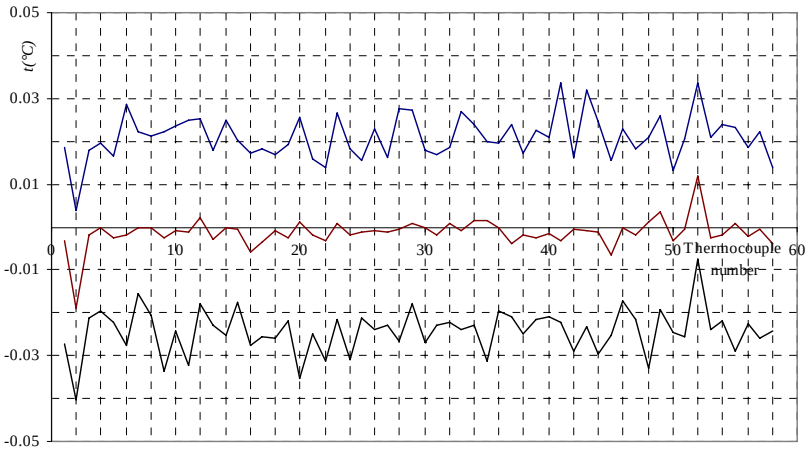

Fig. 3.3. Maximum, average and minimum temperature of all the 58 thermocouples, before calibration.

The average temperature deviation of each thermo-couple (from 0°C) was calculated and the reading of each thermocouple was re-adjusted to give zero value (in the HP-Vee program). The maximum and minimum readings were well within ± 0.04 °C and the standard deviations, calculated with the following equation, were 0.01°C for all temperatures.

$$\text{Standard deviation, } \sigma = \sqrt{\frac{1}{N-1}\sum_{i=1}^{N}(x_i - \bar{x})^2} = 0.01°\text{C} \qquad (3.1)$$

$$\text{Mean valve (average value), } \bar{x} = \frac{1}{N}\sum_{i=1}^{N} x_i \qquad (3.2)$$

The temperature of the ice bath was again measured by all the 58 thermocouples after adjusting the HP-Vee program during a 25 minutes period in 5 seconds intervals. The maximum, average and minimum temperature of each of the thermocouples (after temperature adjustments) during the period are shown in Fig. 3.4. Except for very few numbers, all other temperature readings were well within ± 0.03 °C and the standard deviations were 0.01°C.

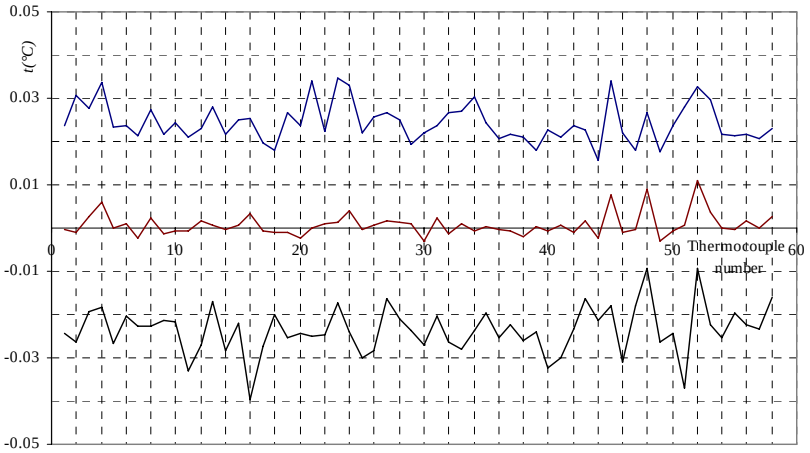

Fig. 3.4. Maximum, minimum and average temperature of each of the thermocouples after adjustment for temperature deviations of the thermocouples in the HP-Vee program.

The maximum error of the measured temperatures was taken as *±0.04* °C.

3.2 Pressure measurements

Druck PDCR 4000 and 2000 series high performance millivolt output pressure transducers were used for all tests. The sensor at the heart of each transducer is a micromachined silicon diaphragm. Data given by the manufacturer for the pressure and differential pressure transducers are shown in Table 3.2.

Table 3.2. The details of the pressure transducers and differential pressure transducers supplied by manufacturer.

Measurement	Number	Range	Voltage supply	Accuracy (combined effect of non linearity, repeatability and hysteresis)
Evaporator pressure	PCDR4061 S/N 1290898	0 - 20 bar	10	*±0.04%*
Condenser pressure	PCDR4060 S/N 1290897	0 - 20 bar	10	*±0.04%*
Evaporator differential pressure	PCDR2160 S/N 777049	0 - 700 mbar	10	*±0.06%*
Condenser differential pressure	PCDR2160 S/N 1092928	0 - 350 mbar	10	*±0.06%*

The circuit diagram of the absolute pressure transducers (abs. PT), differential pressure transducers (DPT) and flow meters in the test-rig is shown in Fig. 3.5. A 10V DC was supplied to each of the pressure transducers. The output millivolt signals from the pressure transducers were connected to the CH17 to CH20 of a 20-channel multiplexer as shown in Fig. 3.5.

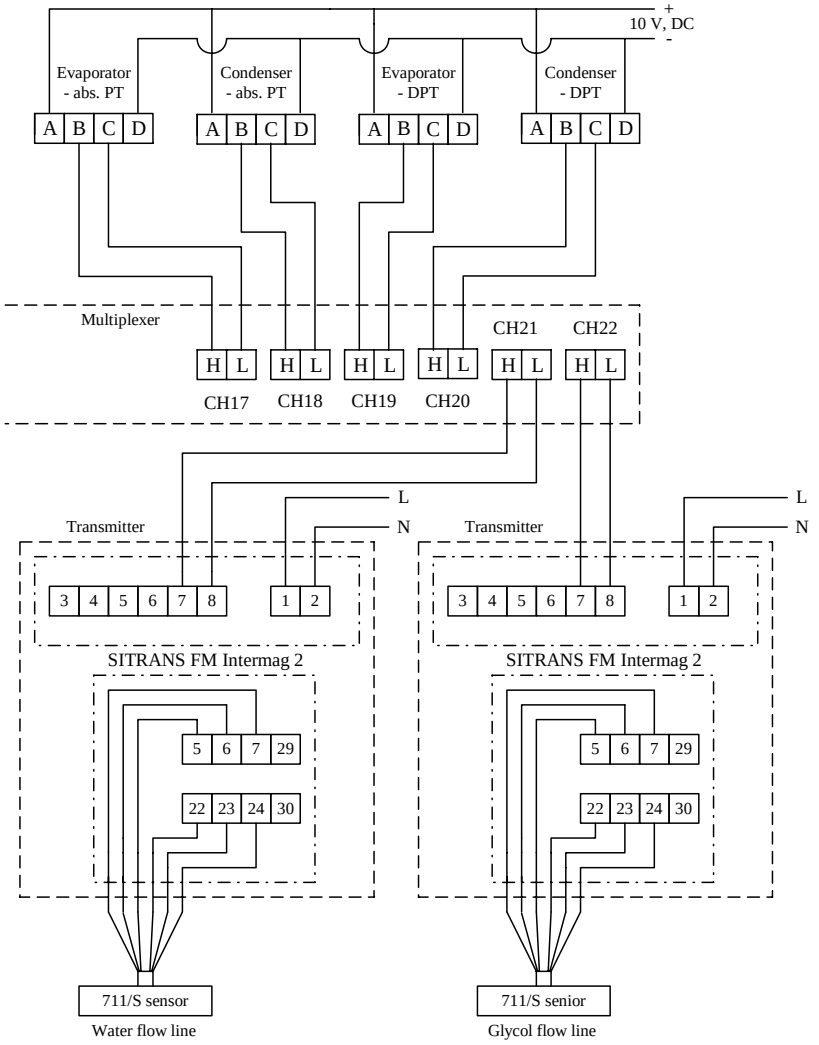

Fig. 3.5. Circuit diagrams of absolute pressure transducers (abs. PT), differential pressure transducers (DPT) and flow meters.

3.2.1 Pressure calibrations

All the absolute pressure transducers and differential pressure transducers were calibrated before each of the experiment against the digital multimeter PREMA 5000. The digital multimeter PREMA 5000 was calibrated by accredited laboratory (AMTELE AB, Huddinge) in Sweden. Laboratories are accredited by the Swedish board for accreditation and conformity assessment (SWEDAC) under the terms of Swedish legislation. The accredited laboratory activities meet the requirements in SS-EN ISO/IEC 17025(2000). Also, some of the differential pressure transducers were calibrated by the previously mentioned laboratory. The pressure transducers and differential pressure transducers were calibrated connecting at their real measuring locations in the test-rig. When calibrating the differential pressure transducers, the negative pressure port of the differential pressure transducer was opened to the atmosphere and the positive port was connected to the test-rig at its measuring location. The accuracy of the calibrator (PREMA 5000) was 0.02% of the readings.

3.2.2 Calibration lines

Calibration lines obtained for the pressure and differential pressure transducers for the final experiments conducted with the test facility are shown in Figs. 3.6 - 3.9. Atmospheric pressure reading of the calibration day was taken from the official measurements at Bromma airport in Stockholm.

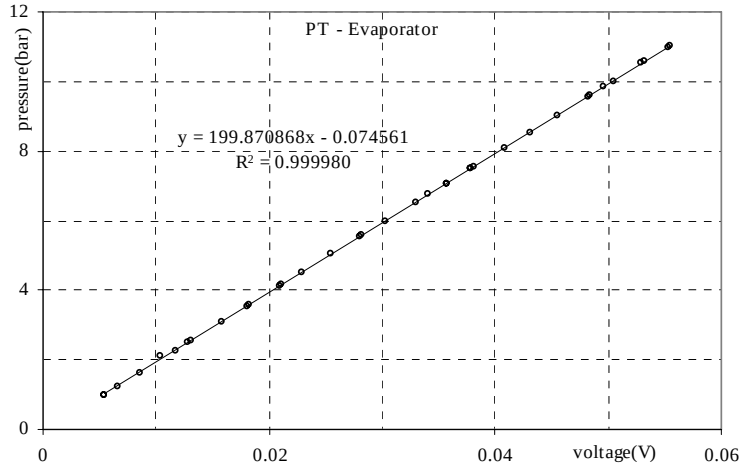

Fig. 3.6. Calibration line for the pressure transducer PCDR4061; S/N 1290898.

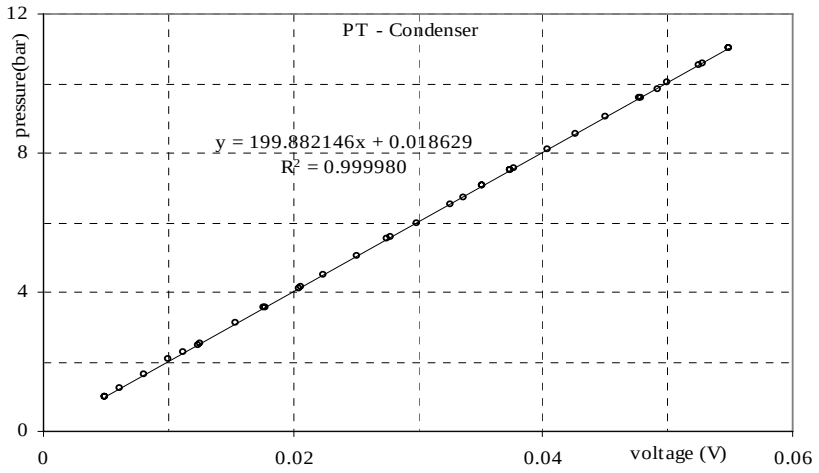

Fig. 3.7. Calibration line for the pressure transducer PCDR4060; S/N 1290897.

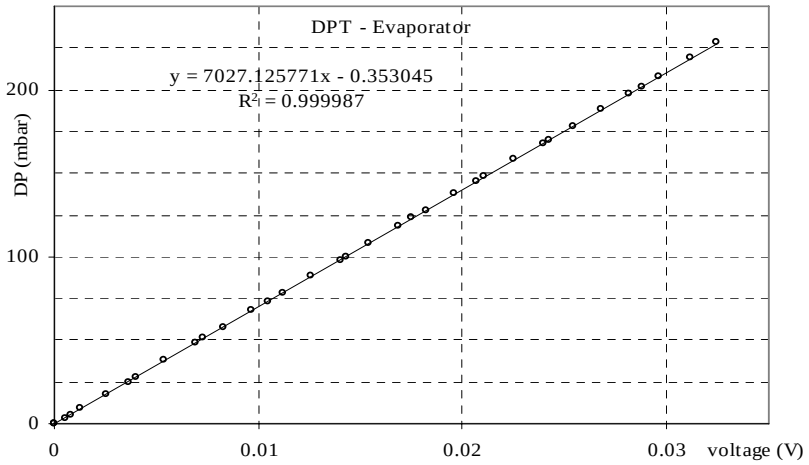

Fig. 3.8. Calibration line for the differential pressure transducer PCDR2160; S/N 777049.

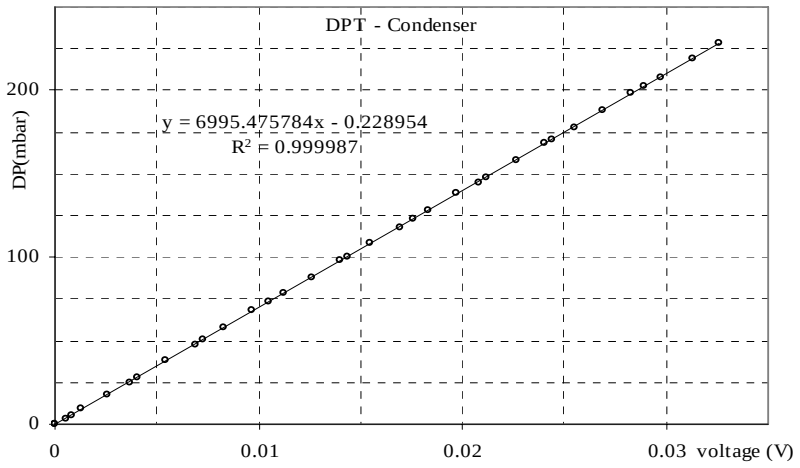

Fig. 3.9. Calibration line for the differential pressure transducer PCDR2160; S/N 1092928.

There were no apparent deviations between calibration curves of the pressure transducers found for the initial experiments and those for the final experiment. Due to limitations in the digital multimeter PREMA 5000, the maximum calibrated pressure of the absolute pressure transducers were about 11 bars. However, the condenser pressure measurements in the experiments were taken up to 20 bars. The accuracies of the pressure transducers and differential pressure transducers were *±0.02%* of the measured value (since the pressure transducers were calibrated frequently, only the uncertainty of the calibrator was considered).

3.3 Flow measurements

Secondary refrigerants (water and glycol) flow measurements were taken by Siemens magnetic-inductive flow transmitters (SITRANS FM Intermag 2) in conjunction with electro-magnetic flow sensors (SITRANS FM 711/S). According to the manufacturer, electromagnetic flow meters are suitable for measuring flow of almost all electrically conducting liquids, pastes and slurries. A prerequisite is that the medium must have a minimum conductivity of 3 μScm^{-1}. The temperature, pressure, density and viscosity have no influence on the result. The analog output signal range of the transmitter was 4 - 20 mA for a flow between 0 and the adjusted maximum flow rate in the transmitter. The Intermag 2 can be used for medium flow speeds up to 12 ms^{-1}. The accuracies of the flow meters are ±0.5% of the measured value for flow rates greater than 0.25 ms^{-1} and ±0.0025 ms^{-1} for flow rates less than 0.25 ms^{-1}. Any value between 0.25 and 12 ms^{-1} can be chosen as the upper range value of the flow meter. The analog signal output 4 - 20 mA linearly displayed the

flow rate between 0 - maximum-adjusted-value. The details of the magnetic-inductive transmitters and flow sensors are shown in Table 3.3.

Table 3.3. Details of the magnetic-inductive transmitters and flow sensors.

		Connected to evaporator glycol flow	Connected to condenser water flow
SITRANS FM Intermag 2	Order number	7ME5033-0AA11-1AA0	7ME5033-0AA11-1AA0
	F-Nr.	N1-N810-8201298	N1-N810-8201294
	Serial-No	2002-307742/A01	2002-307742/A02
	Communication	4 - 20 mA	4 - 20 mA
SITRANS FM MID Sensor 711/S	Order number	7ME5410-1DA10-0BA0	7ME5410-1DA10-0BA0
	Serial-No	2002-307742/A01	2002-307742/A02
	Nominal diameter (DN)	15 mm	15 mm
	ZPH/CFH	0.0 / 528.24	0.0 / 517.15

The flow measurements of the experiments were taken in litres per minute. If the upper range value of the flow sensors were set to its maximum (12 ms^{-1}), the flow meters were capable of measuring a maximum flow rate of approximately 128 $lmin^{-1}$. The output current signals of the flow meters were connected to CH21 and CH22 of a 20-channel multiplexer as shown in Fig. 3.5. The upper range value of the flow meters were set to 3.77 ms^{-1} when they were used for measuring the glycol flow through the evaporator and the water flow through the condenser in the test facility and that gave the maximum possible flow rate measurements of the flow meters of 40 $lmin^{-1}$. When the flow meters were used for single-phase experiments, the set value of one of the flow meters was increased to 7.54 ms^{-1} and that gave the maximum possible flow rate measurement of that flow meter of approximately 80 $lmin^{-1}$. All electrical and piping connections and set values of the flow meters were done according to SITRANS FM Intermag 2 flow transmitter operating manual (order No. A5E00102775-02).

The flow meters were tested with known values and these tests confirmed the accuracies given by the manufacturer.

4 Uncertainty and Random Error Analysis

Introduction

In this section, the theoretical background of the uncertainty analysis is presented. The uncertainty analysis of *Paper V, VI* and *VII* are presented in **APPENDIX A, B** and **C**, respectively.

{This chapter was prepared from the lecture notes of the Measurement Technique course given at the Department of Energy Technology in 2006 (4A5001) and a document presented by professor Per Fahlén [1]. Most of the references were taken from his lecture notes}

The errors that occur when performing experiments can be categorised as systematic errors and random errors as mention in the previous section. The systematic errors can be eliminated or minimised by calibration of the measurement equipment. Random errors are however harder to eliminate, they arise by both the physical quantity that is being measured, and the measurement equipment. Random errors can occur for a variety of reasons. They may occur due to lack of sensitivity. For a sufficiently small change an instrument may not be able to discern it. They may occur due to noise and vibrations or extraneous disturbances which can not be taken into account. Random errors displace measurements in arbitrary direction whereas systematic errors displace measurements in a single direction. Random errors are unavoidable and must be lived with.

4.1 Standard deviation

The standard deviation is the most common measure of statistical dispersion. Simply put, standard deviation measures how spread out the values in a data set are. More precisely, it is a measure of the average difference between the values of the data in the set. If data points are all similar, then the standard deviation will be low (close to zero). If the data points are distance measurements in meters, the standard deviation also is measured in meters. There are two common formulas used for computing standard deviation in the literature.

The standard deviation of a population is given by,

$$\sigma = \sqrt{\frac{1}{N}\sum_{i=1}^{N}(x_i - \bar{x})^2} \tag{4.1}$$

The standard deviation computed from a sample of the population is given by,

$$\sigma_x = \sqrt{\frac{1}{N-1}\sum_{i=1}^{N}(x_i - \bar{x})^2} \tag{4.2}$$

where, the mean value (average value) is given by,

$$\bar{x} = \frac{1}{N}\sum_{i=1}^{N} x_i \tag{4.3}$$

The uncertainty of the mean value (standard error of the mean), $\bar{x}$ is expressed by the standard deviation of the mean,

$$\sigma_{\bar{x}} = \frac{\sigma_x}{\sqrt{N}} = \sqrt{\frac{1}{N(N-1)}\sum_{i=1}^{N}(x_i - \bar{x})^2} \tag{4.4}$$

Given only sample values $x_1,\ldots\ldots x_N$ from some large population, many authors define the sample standard deviation by Eq. (4.2). The definition of standard deviation in Eq. (4.2) is called the unbiased estimator of the underline population.

In the experiments reported here, the standard deviation was calculated by Eq. (4.2). However, if sample data are large, the difference between the standard deviations calculated by Eq. (4.1) and Eq. (4.2) are negligibly small.

The meaning of standard error is that if the measurements of variable x were repeated there is a 68% probability that each new value would lie within $\bar{x} \pm \sigma_{\bar{x}}$ .The probability density function of a normal distribution with mean value $\bar{x}$ and standard deviation σ is shown in Fig. 4.1.

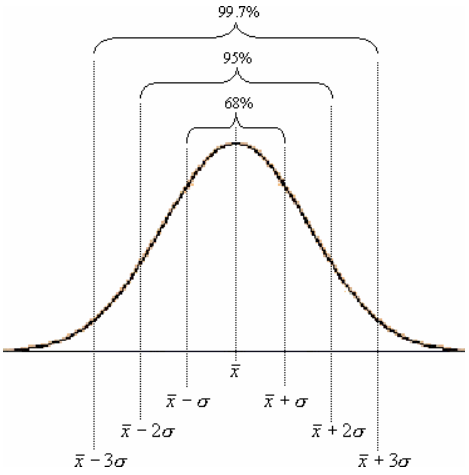

Fig. 4.1. Plot of the probability density function of a normal distribution with mean value $\bar{x}$ and standard deviation σ.

Some notable qualities of the normal distribution:

- The density function is symmetric about its mean value.
- 68.26894921371% of the area under the curve is within one standard deviation of the mean.
- 95.44997361036% of the area is within two standard deviations.
- 99.73002039367% of the area is within three standard deviations.
- 99.99366575163% of the area is within four standard deviations.
- 99.99994266969% of the area is within five standard deviations.
- 99.99999980268% of the area is within six standard deviations.
- 99.99999999974% of the area is within seven standard deviations.

Finally the uncertainty due to random errors, stated with a specified confidence level, is calculated according to (Swedish standard SS 01 41 50) [1, 2]:

$$r = t_\beta \sigma_{\bar{x}} \tag{4.5}$$

The factor t in Eq. (5) depends on the desired confidence level $\beta\%$. For example, 95% confidence level, in the case of large number of values corresponds to $t_{95} = 1.96 \approx 2$, also known as 2σ limit.

4.2 Combinations of components uncertainty

Random errors are normally stated as "type A" errors. Systematic errors are normally stated as "type B" errors.

The combination of different components ("type A" and "type B" errors) of measuring uncertainty is different according to different standards. According to BIPM/ISO (International Bureau in Paris) [1], components of uncertainties of "type A" and "type B" may be considered to be independent and when this is the case the combined uncertainty $U_{\bar{x}}$ may be computed as,

$$U_{\bar{x}} = \sqrt{\sigma_{\bar{x}}^2 + w_{\bar{x}}^2} \tag{4.6}$$

Assuming rectangular distribution, the uncertainty of systematic errors (type B) transform into standard deviations by the following formula,

$$w_{\bar{x}} = \frac{a}{\sqrt{3}} \tag{4.7}$$

where "a" is the maximum deviation of the rectangular distribution.

Prior to any combination of uncertainties it is recommended to make uncertainty "type B" symmetric. The expression (4.6) provides a combined uncertainty at a confidence level corresponding to 1σ (68%). The confidence level 68% is usually not satisfactory and 95% confidence level is considered. Therefore, a factor called coverage factor (k) is introduced. This factor, in some sense, corresponds to the Student t-factor relation to the normal distribution. Then, the overall uncertainty is computed as,

$$U_{\bar{x}} = k\sqrt{\sigma_{\bar{x}}^2 + w_{\bar{x}}^2} \tag{4.8}$$

where, k is a numerical factor which normally is assigned a value in the range 2-3. For instance $k = 2.5$ according to SS 2620 [1, 3] or $k = 2.0$ according to WECC [1, 4], EAL [1, 5] and SWEDAC (Swedish Board for Technical Accreditation).

In most cases it is not possible to measure the desired output directly, but it can be determined indirectly by means of some physical relationship. For example, assume the desired physical quantity is a function of several other quantities x_1, …. x_n, i.e.

$$y = f(x_1, \ldots x_i \ldots \ldots x_n) \tag{4.9}$$

Assuming all x_i are independent variables, then the uncertainty of y is estimated by [1],

$$\text{Type A: } \sigma_y = \sqrt{\sum_{i=1}^{n} \left(\frac{\partial f}{\partial x_i} \sigma_{\bar{x}_i} \right)^2} \tag{4.10}$$

$$\text{Type B: } w_y = \sqrt{\sum_{i=1}^{n} \left(\frac{\partial f}{\partial x_i} w_{\bar{x}_i} \right)^2} \tag{4.11}$$

Then the "type A" and "type B" uncertainty combines as,

$$U_y = \sqrt{\sigma_y^2 + w_y^2} \tag{4.12}$$

Expression (4.12) gives the overall uncertainty at confidence level 68%. For better confidence level the expression (4.12) can re-written as,

$$U_y = k\sqrt{\sigma_y^2 + w_y^2} \tag{4.13}$$

$k = 2$ gives the uncertainty at confidence level of 95.45% and $k = 3$ gives the uncertainty at confidence level of 99.73%.

References

[1] Analysis of Measurements - Uncertainty, concepts and procedures, Per Fahlén, Visthusgatan 6, SE-504 44 Borås, Sweden (01KTHUnceratnity 1: Per Fahlén 01-10-01), 2001.

[2] Svensk standard - Metrologi - Anggivande av mätresultat (Standardisering kommissionen i Sverige, Stockholm, Sweden), SS 014150, 1981.

[3] Värmeutrustning – Värmepumpar – Fältprovning och prestandaredovisning (Sveriges Mekanstandardisering, Stockholm, Sweden), SS 2620, 1988.

[4] Guidelines for the expressions of the uncertainty of measurements in calibrations (Western Europe Calibration Conference), Doc 19-1990, WECC, 1990.

[5] Expression of the uncertainty of the measurement in calibration (European Corporation for Accreditation of Laboratories), EAL-R2, 1997.

5 Conclusions and Suggestions for Future Work

5.1 Conclusions

The heating energy demand of a new single-family European house is generally in the range of 100 - 150 kWh/(m^{2}yr). However, it could be lower or higher than the given range depending on the conditions of the house. A heat pump with the heating capacity of 5 kW could be able to provide full or part of the heating need of a single-family house. Heat pumps of this size generally give average COP1 higher than 3 and this value could be further increased by proper selection of components, use of high temperature level heat sources and low temperature level heating systems, etc. The ground as heat source and floor heating systems are encouraged to obtain higher COPs and stable operations of the heat pump during a heating period.

The refrigerant is one of the most important elements of any heat pump and refrigeration system, since it greatly affects the efficiency of the system and compatibility with the environment. The ozone depletion potential (ODP) and global warming potential (GWP) of commonly used refrigerants are considered as major environmental problems. Safety is the other major concern for refrigerants. Many synthetic refrigerants are considered as excellent candidates if their high ODP and GWP are neglected. Particularly, environmental effects of synthetic substances are still a concern due to the many possible unknown effects and, therefore, research interest has been more focused on applications of well characterized natural refrigerants. Although environmental concerns and safety issues are forcing major shifts from traditional choices of refrigerants, other aspects are also being considered in selecting a suitable refrigerant for a particular refrigeration application.

Propane is a natural refrigerant that does not have any ozone depletion potential and has a very low global warming effect compared to most commercially available refrigerants. It is non toxic, chemically stable while inside the refrigeration system, compatible with most materials

used in HFC equipment and miscible with commonly used compressor lubricants. Propane has very good thermodynamic and transport properties that closely resemble those of HFC refrigerants, making it possible to use with well known technologies. However, the main concern with propane is its high flammability. To decrease risk, refrigeration and air conditioning systems using propane should be designed to operate with small refrigerant charges and zero refrigerant leaks.

This project has shown that, it is possible to design a heat pump for the typical requirements of a single-family house giving high COP and operating with low refrigerant charge. The project has focused on the design of heat exchangers with small internal volume. The reported results show that the minichannel heat exchangers have better heat transfer performances compared to plate heat exchangers or heat exchangers with large diameter channels. This allows designing more compact and safer refrigeration equipment with high performances.

The high solubility of propane in most compressor lubrication oils should be considered when selecting lubrication oil for propane refrigeration compressors. Generally, it is recommended to use lubrication oil with higher viscosity grades for propane than with R22 for proper lubrication. Several oils were proposed for use with propane by some lubricant manufactures. *Select Lubricants* has recommended SL18-Series (Synthetic hydrocarbon base) and SL34-Series (Polyoxyalkylene Glycol) compressor lubrication oils for use with natural gas and propane. *CPI Engineering Services* has recommended CPI-1518-Series (polyglycols based) for propane compressors. Tests showed that propane is much less soluble in PAG oil than in POE.

The reported heat pump can be operated with about 200 - 230 g of refrigerant propane, giving over 5 kW heating capacity at typical Scandinavian heat source/sink temperature levels. Further reduction in the charge is possible by use of less soluble oil, by using compressors with lower oil charge and/or smaller internal volume and by redesigning the end caps of the aluminium tube heat exchangers. Since propane is highly soluble in compressor lubrication oil, the amount of refrigerant that could rapidly escape in case of an accident or leakage would be less than 150 g.

The experimentally tested scroll compressor, which was originally recommended for refrigerant R407C worked well with refrigerant propane.

5.2 Suggestions for future work

The available correlations and models to predict boiling and condensation heat transfer of minichannel heat exchangers are still inadequate, es-

pecially, for low refrigerant mass flux rates (lower than 100 kgm^{-2}). Even the correlations available in the literature for single-phase heat transfer of minichannel heat exchangers are not univocal. Many models in the literature cannot be applied for actual heat exchangers due to their limitations. For example, many correlations are only applicable for fully developed flows. However, in many practical heat exchanger applications it is hard to find fully developed flows.

Generally, there is lack of heat transfer information regarding small channel heat exchangers in the literature. The reliability and uncertainty of data also is a concern in small scale heat transfer. For example, the method employed in this work to calculate the heat transfer coefficient would not be the best solution to predict very accurate heat transfer coefficients in minichannel heat exchangers involving small flow rates or small temperature differences, etc. due uncertainties. The calculated refrigerant side heat transfer coefficients of minichannel heat exchangers in this work was based on the following equation,

$$\frac{1}{UA} = \frac{1}{\alpha_1 A_1} + \frac{\delta_t}{k_t A_m} + \frac{1}{\alpha_2 \left(A_b + \xi A_f\right)} \tag{5.1}$$

Rearranging equation (5.1),

$$\alpha_1 = \frac{1}{\left(\frac{\delta_t}{k_t A_m} + \frac{1}{\alpha_2 \left(A_b + \xi A_f\right)} - \frac{1}{UA}\right) A_1} \tag{5.2}$$

According to equation (5.2), the refrigerant side heat transfer coefficient (α_1) is a function of several parameters such as tube thickness (δ_t), thermal conductivity of the tube material (k_t), mean area of the tube wall (A_m), secondary refrigerant side heat transfer coefficient (α_2), base area (A_b), fin efficiency (ξ), fin area (A_f), area of the tube-side (A_1) and overall heat transfer coefficient (U). The uncertainty of the calculated refrigerant side heat transfer coefficient would be very high due to the uncertainty of all the above parameters. Alternatively, the heat transfer coefficient of the refrigerant side can be calculated if the wall temperatures are measured. Then the refrigerant side heat transfer coefficient can be expressed by the following expression,

$$\alpha_1 = \frac{\dot{Q}}{\Delta t A_1} \tag{5.3}$$

According to equation (5.3), the refrigerant side heat transfer coefficient (α_1) is a function of only three parameters: Heat transfer rate ($\dot{Q}$), wall-to-refrigerant temperature difference (Δt) and area of the tube-side (A_1). Since few parameters are involved in the second case, the accuracy of the calculated heat transfer coefficients could be better than by the method involved to calculate heat transfer coefficients in this report by Eq. (5.2).

Therefore it is suggested to do research on heat transfer (single-phase, evaporation and condensation) in minichannel tube heat exchangers, which are made by various available geometrical shapes, by measuring wall temperatures. The heat exchangers are suggested to be connected to experimental test facilities simulating real refrigeration and heat pump systems.

Information on refrigeration compressors and lubrication oils in the literature is not well established. Therefore it is suggested to do research on compressors and compressor lubrication oils.

In the concern of refrigerant charge reduction and better refrigerant distribution inside the heat exchangers, the inlet and exit ports of the heat exchangers are playing an important role. However, very little or no research was conducted regarding refrigerant inlet and exit ports of the heat exchangers in the literature. Therefore it is suggested to test various inlet geometries in future tests.